Sheffield Hallam University

The role of migration in a spatial extension of the Webworld eco-evolutionary model

ABERNETHY, Gavin <http://orcid.org/0000-0001-6983-6349>, MCCARTNEY, Mark and GLASS, David H

Published version

Copyright and re-use policy

The Role of Migration in a Spatial Extension of the Webworld Eco-evolutionary Model

Dr Gavin M Abernethy[a,b], Dr Mark McCartney[a], Dr David H Glass[a]

[a]*School of Computing, Ulster University, UK*
[b]*Department of Engineering and Mathematics, Sheffield Hallam University, UK*

Abstract

We extend an eco-evolutionary food web model to a spatially-explicit metacommunity model which features migration of populations between multiple local sites on the same time-scale as feeding and reproduction. We study how factors including the implementation and rate of dispersal, properties of the local environments, and the spatial topology of the metacommunity interact to determine the local and global diversity and the degree of synchronisation between local food webs. We investigate the influence of migration on the stability of local networks to perturbation, and simulate a 5×5 spatial arrangement of cells, demonstrating that combining adaptive migration and heterogeneous habitats allows distinct food webs to coevolve from the beginning of the simulation. When coupling food webs by diffusion migration after an initial period of isolation, the Webworld model can construct metacommunities of distinct food webs if the local sites have spatially-homogeneous environmental parameters. If the sites have heterogeneous parameters, synchronisation between food webs increases greatly, but this can be offset by a greater number of sites and less-connected spatial topologies.

1. Introduction

Understanding of food web functioning and maintenance has been imbued with renewed significance in recent decades, as biodiversity loss, pollution, climate change, conservation and other issues regarding the anthropological impact on natural communities made its way to the forefront of both public consciousness and the interests of the scientific community. Mathematical models are a means of understanding and predicting ecological changes, in order to mitigate or recover from their potentially devastating effects [May09, McC00, DALP09]. Eco-evolutionary models have recently become popular in computational ecological modelling, studying the interrelated effects of evolutionary and ecological processes within a single simulation. These can often feature arbitrary numbers of species, with their trophic relationships emerging as a result of the feedback between the two processes. Successful examples include the model by Loeuille and Loreau [LL05] that delineates species by a single continuous trait (body size), the three-parameter adaptation of this model [ARRDG15], and the eco-evolutionary extension of the Niche Model [GD08]. The Webworld model [CHM98, DHM01] is another well-known example, combining foraging, ecological processes (feeding and reproduction), and evolutionary processes (mutation and speciation) on three distinct but interlinked timescales. Species are defined by an allocation of a number of discrete features, each of which are scored against every other feature, which determine the existence and strength of competition between species, as well as the strength and direction of feeding relationships. Speciation is then represented by introducing a mutant with a small population that retains all but one of the parent's features, with the other having been randomly replaced. Iterating the population dynamics of the system, which incorporates a sophisticated multi-predator multi-prey ratio-dependent functional response, determines whether or not this new species is able to establish itself in the food web. A number of studies have continued to develop the Webworld model, examining the structure, stability and statistical properties of the food webs it generates in some detail, as well as testing the effects of various changes to the parameters and modelling choices involved [DMQ04, QHM05a, QHM02, QHM05b, LM08a, LM08b, McK04]. In our other work [AMG19], we reproduced the model and performed additional tests, investigating the link-species relationship, network properties, and stability (in the sense of robustness) demonstrated by its food web networks.

A second area that has seen much interest is metacommunity and spatial modelling [LHM+04]. When considering the effect of dispersal rates between patches on the diversity and stability of the local food webs, the general consensus that emerges is of a unimodal relationship governed by "the balance between the positive effects of low dispersal (allowing recolonisation and rescue effects) and the negative effect of high dispersal (synchronisation)" [HGHL10], as highlighted in the studies by Mouquet and Loreau [ML02, ML03]. A recent study that spatially-connected four sites featuring food webs generated by the Niche Model found that even at very low dispersal rates (modelled by stochastic events), stability in the sense of species persistence was increased by increasing the rate of these rare movements [TD18]. The spatial topology of how these patches are connected was generally found to make little difference. Other examples of metacommunity models include the 2008 incarnation of the

---

Matching Model featured invasion from nearby communities [RIAI08]. Hauzy and others studied the effects of the dispersal rate between two patches in a Rosenzweig-MacArthur model with one predator and one prey species [HGHL10]. Hamm and Drossel [HD17] constructed a metacommunity of twenty connected food webs using Holling Type-II population dynamics on Niche Model topologies. One straightforward framework for a spatial model is the coupled map lattice (CML). Simple implementations in one dimension have been carried out using two coupled logistic maps to model a single species that migrates between two regions [Llo95, Fro92]. In two dimensions, CMLs divide a geographic region into cells in which the local dynamics are calculated at each time step, followed by a migration stage where populations may transfer between adjacent cells. Examples of such efforts have been applied to systems of plants [HMW96] and insects [HCM91], predator-prey relationships with more than two species [MAGM16], and a two-dimensional lattice using the generalised Lotka-Volterra equations [SBV92],Holling Type II [HZ16], or Beddington-deAngelis [HZY+17]. These works focused on both mathematical bifurcation analysis, and uncovering spatial pattern formation in the system by means of numerical simulations across a $n \times n$ region where n could be as large as 200 in the data presented.

Recent efforts have begun to integrate these two approaches and create metacommunity models with an evolutionary perspective. Loeuille and Leibold [LL08] studied a multispecies metacommunity with evolution where one of the habitats also varied temporally, testing the effect of the relative rates of adaptation, dispersal, and environmental fluctuation on the resulting species compositions. In most cases, the changing environment resulted in invasions before the resident species could adapt, but sufficiently low relative rates of migration allowed adaptable species to gain an uninvadable monopoly on local environments, and if the rates of evolution and migration were both high relative to environmental fluctuation then a single species could potentially dominate the entire metacommunity. Allhoff et al developed a spatial version of the Loeuille-Loreau eco-evolutionary model [AWRD15], considering both an environment of two patches and a chain of eight patches, where migration between the neighbouring regions could occur either from the beginning of the evolutionary simulation or after a set period of time had passed. They also investigated several means of modelling the migration process itself, whether diffusive, allometrically scaled with body size (large species travel faster), or only occurring when the species' population was decreasing in its current environment (which can simultaneously model a lack of food or a predatory pressure without having to assign relative weightings to these factors). These simulations demonstrate two possible outcomes: rapid migration causes the species networks of the different regions to become effectively identical, and slow migration may increase local diversity by producing a network of food webs that are very similar in trophic structure, but the primary species in a given trophic level may differ between the regions, with each also featuring a very small population (maintained only by migration) of the dominant species in the corresponding trophic level of the neighbouring networks. However, in order to obtain heterogeneous food webs, it was necessary to incorporate adaptive migration, and not allow the food webs to co-evolve from the very beginning of the simulation.

Some of the same authors undertook a similar analysis of a spatial version [BDA17] of their own model that could be considered a variant of the Loeuille-Loreau model with additional evolving traits. This spatial study considered size-dependent migration between metacommunities of either two or four habitats (comparing ring and star topologies for the latter), varying the times during which migration was permitted. They demonstrated that on evolutionary timescales incorporating a spatial aspect increased diversity compared to the single-region version of the model, through a rescue effect of the low-population top predators which led to top-down effects that increased diversity at every trophic level. The spatial topology could be important, as irregular topologies created a disparity between the food web structures in the central and satellite patches resulting in even greater diversity compared to regular spatial arrangements. Furthermore, networks were found to have a memory effect, such that habitats that were no longer connected to others would still retain a larger number of species for the duration of the simulation.

Investigations of spatial eco-evolutionary modelling is still in its infancy. For example, the studies above ultilised more sophisticated forms of migration such as adaptive migration, and in other experiments coupled inhomogeneous environments, but did not combine the two. In this work, we have extended our previous study [AMG19] of the Webworld eco-evolutionary model to a spatially-explicit metacommunity, modelled as a two-dimensional coupled map lattice of local food webs with migration of populations between them occurring on the same timescale as population dynamics (feeding and reproduction). We shall compare the results of coupling homogeneous and heterogeneous environments, investigate the significance of spatial topology in this model, vary the frequency of movement between coupled cells for diffusion, stochastic and adaptive migration, and combine these features in a large metacommunity simulation that coevolves from the beginning. Of particular interest to us will be the global and local diversity of the patches, the degree to which the local food webs are synchronised (possessing the same collection of species), and the interaction between migration and measures of network stability.

2. Description of the model

We describe our spatial version of the model here in detail. For full justification of each step, refer to the original paper by Drossel, Higgs and McKane [DHM01].

2.1. Model initialisation

1. Draw trait scores for a 500x500 antisymmetric array β with zeros on the diagonal and all other scores drawn from a Gaussian distribution with mean 0 and variance 1.

2. For each local cell that is to have a unique resource species, draw 10 distinct traits. The resource begins with a population equal to R/λ, where R is the resource biomass and λ is the ecological efficiency (the ratio of the predator's biomass gain to the prey's biomass loss) and kept at 0.1 throughout. Both are parameters for the simulation.

3. For each cell which is to have its own initial (non-resource) species, draw 10 distinct traits. The first species begins with the population (or equivalently, biomass) equal to 1.0, which is the minimum population size allowed. If a non-resource species falls beneath this threshold during any point in the ecological dynamics, it is considered extinct and its population is set to zero.

4. Begin the evolutionary timestep loop. At each timestep, the ecological loop is iterated and then a single speciation event occurs in one of the local food webs. We typically perform 100 000 evolutionary timesteps multiplied by the number of cells, so that each cell will on average undergo 100 000 speciation events, and the simulations can be compared to previous studies of single cell systems that usually underwent 120 000 evolutionary timesteps.

2.2. Iteration of the model

Each evolutionary timestep consists of iterating the ecological timesteps described below until either a steady state (fixed point or cycle up to period 10) is reached within a tolerance of 1.0, or a maximum of 100 000 ecological timesteps have been performed. After either of these conditions has been met, a speciation event takes place. This involves selecting a species and local population with probability proportional to its population, so that speciation occurs in a particular locale. Cells with very low diversity will be less likely to be the location for a speciation if they have lower cumulative non-resource populations than other cells, however this mechanism does reduce the potential disparity compared to choosing parental species with equal probability. In such a case, in disconnected spatial scenarios, it would be possible for one cell's species diversity to grow exponentially while leaving the others with a small number of species who are consistently not chosen as a parent.

A child species with population 1.0 is introduced, and the parent population is reduced by 1.0, in the same cell. The child species retains 9 of the parents' 10 traits, while one trait is randomly selected and exchanged for a random trait other than the 9 currently possessed. If the new trait set matches another species that already exists in the metacommunity, then a population size of 1.0 is simply exchanged between the parent and this species in the cell where mutation is occuring.

An ecological timestep consists of the following process for feeding and reproduction for each species, followed by movement if applicable:

1. Alternately iterate the "foraging timestep" between the following two steps (a) and (b), until either a fixed point is reached with tolerance 0.1 or a maximum of 100 000 foraging timesteps have been performed.

   (a) For each predator i, distribute the foraging efforts (if it is the first timestep, distribute them equally amongst possible prey), according to the equation:

   $$f_{i,j} = \frac{g_{i,j}}{\sum_{k \in Prey} g_{i,k}} \tag{1}$$

   (b) For each predator i, update their ratio-dependent functional responses $g_{i,j}$ for each prey j according to the equation:

   $$g_{i,j} = \frac{S_{i,j} f_{i,j} N_j}{b N_j + \sum_{k \in P_j} \alpha_{i,k} S_{k,j} f_{k,j} N_k}, \tag{2}$$

   where:
   - b is a saturation parameter, which scales feeding scores in the simulation.
   - $S_{i,j}$ is the non-negative trait score of i against j. It is calculated as an average of the scores of i's traits against j's traits, and so

   $$S_{i,j} = \frac{1}{10} \sum_{m=1}^{10} \sum_{n=1}^{10} \beta_{u_m, v_n}, \tag{3}$$

   where u_m is the mth trait of species i and v_n is the nth trait of species j.
   - P_j is the set of species who are predators of j.

3

- $\alpha_{i,k}$ is the symmetric competition strength of i against k. This is calculated using the equation $\alpha_{i,k} = c + (1-c)q_{i,k}$, where c is our competition parameter describing how the strength of interspecific competition tails off between biologically-distinct species, and $q_{i,k}$ is the fraction of traits shared between species i and k.

2. Update the local populations, as a result of feeding and reproduction, using the Euler method with step size 0.2, according to the balance equation:

$$\frac{\mathrm{d}N_i}{\mathrm{d}t} = -N_i + \lambda \sum_{j=0}^{n} N_i g_{i,j}(t) - \sum_{k=1}^{n} N_k g_{k,i}(t), \tag{4}$$

where the terms on the right-hand-side represent species i's natural death rate in the absence of predators, biomass gain due to predation and biomass loss due to being predated upon. Note that this model assumes that natural mortality and metabolic efficiency are uniform across all species, trophic positions, and geographic regions.

3. If movement is enabled at the current time in the simulation, it takes place between connected cells. The population of species i in cell (x,y) is then given by:

$$N_i^{x,y} \mapsto N_i^{x,y} + \sum_{j=1}^{x_{max}} \sum_{k=1}^{y_{max}} \delta_{j,k,x,y} \mu_{i,j,k,x,y} - \sum_{j=1}^{x_{max}} \sum_{k=1}^{y_{max}} \delta_{x,y,j,k} \mu_{i,x,y,j,k} \tag{5}$$

where $\delta_{j,k,x,y} = 1$ if the cells (j,k) and (x,y) are connected and distinct, and zero otherwise, and $\mu_{i,j,k,x,y}$ denotes the amount of the local population of species i in cell (j,k) that migrates to cell (x,y) at this time step. How this is calculated will depend on a number of factors. It is always a function of the population of species i that currently exists in cell (j,k), and in most cases is simply a fraction of this value. However we will employ a variety of alternative migration schemes later in the paper, such as incorporating a random variable to determine when migration takes place, or making $\mu_{i,j,k,x,y}$ a function of the difference between the local population at the current and previous ecological timesteps.

4. Return the resource population to its parameter setting.

2.3. Data collection

For a single simulation run, we collect the following properties. The versions of robustness (defined below) are much more computationally expensive compared to other properties, and so they are usually collected less frequently.

- Number of extinctions between subsequent evolutionary timesteps. The distribution of these event sizes is then produced.

- A representation of the phylogeny of those species which are alive at the end of the simulation, showing the creation time, extinction time, and parent species of each species in the direct ancestral lineage of the final species.

- All of the prey-averaged trophic levels occupied at each output step.

- Average fraction of traits which overlap between pairs of distinct species in the first, second and third (shortest-chain) trophic levels, assuming species exist at these levels.

- The maximum and average prey-averaged trophic level (abbreviated to PATL). Also known as Trophic Height, this is calculated recursively by averaging over the prey-averaged trophic levels of a species' prey, weighted by the fraction of effort that the species devotes to feeding on them until at least 99% of the flow of biomass to each species is accounted for. This cutoff is necessary when using the Webworld model, as feeding loops can occur.

Many food web network properties are often determined using "trophic webs" in order to account for inconsistent empirical sampling effort [Dun06]. In these, any taxonomic species that have the same predator and prey relationships active, and which may therefore appear functionally similar in trophic behaviour, are amalgamated as a single "trophic species". During each simulation, at each output step, we create the trophic network in addition to the taxonomic network in order to record its properties. To do this, we create a binary array of species feeding relationships, only counting those with effort $f > 10^{-6}$ and so they are the feeding relationships which are not merely possible, but actually realised in the simulation. Next, we amalgamate any pairs of species that have the exact same set of prey and predator links. Biomass and population dynamics are excluded from consideration during analysis of trophic webs.

For both taxonomic and trophic webs, we collect the following properties in each cell:

- Number of species, S, in each cell (a.k.a. diversity). Note that for this, and other properties such as link density, the Resource is counted as a species.

- Fraction of Basal (only feeds on the resource), Top (no predators, but not basal), and Intermediate (all other) non-resource species.

- The Link Density (L/S) and Connectance ($2L/S(S-1)$) of the food web. Links are only counted in the taxonomic web if they have effort $f > 10^{-6}$ (which is the minimum value allowed for possible links for computational purposes).

- The maximum and average shortest-chain trophic level (abbreviated to SCTL), which is the length of the shortest path from the species to the resource (e.g. a species which feeds directly on the resource has SCTL equal to 1).

- The fraction of species which are omnivores, meaning that they feed with $f > f_{min}$ on at least two species with different shortest-chain trophic levels.

- The "Local Clustering Coefficient" (abbreviated to LCC), which is the probability that two neighbours of a node are connected, averaged over all species, and also averaged over all non-resource species.

- The "Global Clustering Coefficient" (abbreviated to GCC), which is the probability that a two-path in the food web is closed.

- Five measures of Robustness, which is a form of community stability. To calculate this, first we isolate the cell under consideration by disabling migration if applicable and iterating the ecological loop to remove local populations that cannot sustain themeselves. Then we manually delete species one at a time, iterating the ecological loop in between, until the total number of extinctions (both primary and secondary) is at least half of the non-resource species that remained after isolation. The fraction of non-resource species that had to be manually deleted is then the Robustness.
  - Random - delete species in a randomly-selected order. Average the robustness over 100 deletion sequences.
  - High-C - delete species in order of most-to-least connected (at that moment, rather than how connected they were at the beginning). Where there are multiple options, choose randomly.
  - Low-C - as above, except that we delete species in order of least-to-most connected.
  - High-C Non-basal - delete species in order of most-to-least connected, excluding Basal species. If this is not possible due to only basal species remaining at a point before 50% total extinctions have occured, do not return an answer. Where there are multiple options, choose randomly.
  - Low-C Non-basal - as above, except that we delete non-basal species in order of least-to-most connected.

For taxonomic webs only we collect the following properties:

- The average population (biomass) of each non-resource species in the web.

- Snapshots of the web at various points during the simulation.

- The average and cumulative population throughout the simulation subdivided by Basal-Intermediate-Top classification, and by shortest-chain trophic level.

We also present several properties separated between "shared" species (those which currently maintain populations both in the cell under consideration and in at least one other cell) and "unique" species (which are only present in the cell being considered). During the initial phase of most simulations, when movement between cells is not allowed, all species are unique (except for scenarios where a single resource species is found in all cells). First, we determine the local diversity, average populations, and average and maximum trophic levels in each cell, restricted to the subgroup of shared or unique species. For example, the fraction of unique species which are basal. Then we calculate the fraction of basal, intermediate, top, and omnivorous species in each cell which are shared and the fraction that are unique. These fractions must always sum to unity.

Next we consider data relating to lifespan and species invasions and deaths. In particular, this consists of properties calculated over various time periods for species which could be classified at the appropriate time in the following species groups: Basal, Intermediate, Top (abbreviated BIT), Unclassifiable BIT, Shortest-chain Trophic Level 1, 2, 3, 4, 5 or greater, or unclassifiable shortest-chain trophic level. Sometimes species cannot be classified during the time when this data is collected, as trophic level and BIT classifications are not fixed properties for a given species. These five properties are calculated for each of the ten groups for every 10 000 time step period, and finally over the entire simulation. In all cases, species are only counted if they successfully invaded the system (therefore having lifespan greater than one evolutionary timestep):

- The average evolutionary lifespan (that is, the number of evolutionary timesteps that the species persists) of species born in the time period, and who were most commonly assigned to that species group during their lifetime.

- The number of deaths of species (turnover) that occur during the time period, who were counted as part of that species group at or just before their death.

- The absolute frequency of speciation events during the time period, where the parental species was part of the species group at the time of speciation, and which resulted in the child successfully invading the system.

- The previous property expressed as a fraction of total (successful and unsuccessful) speciation events to parents of the group during the time period. In other words, the rate of successful invasions of children of the species group during that time period.

At the end of the simulation:

- Visually represent the final Food Web.

- Degree distribution of both final Taxonomic and Trophic webs.

3. Comparison of 18 scenarios of multi-cell simulations featuring diffusion migration

We conduct studies of 18 different spatial scenarios. In all cases, the simulation begins with a resource and a single non-resource species in each of the cells, which are all initially disconnected with no movement until it is enabled at a certain time. When migration is permitted, it occurs in the form of diffusion along each link between cells, with a fraction of 0.005 of the local population of each non-resource species in each cell leaving along each link to a connected local cell. Therefore the movement function μ from Equation (3), for the amount of species i which migrates from cell (j,k) to cell (x,y), is given by $\mu_{i,j,k,x,y} = 0.005 \times N_{i,t}^{j,k}$.

In all cases, the following technical details are observed: data is collected every 10 evolutionary timesteps, with the exception of stability tests in the form of robustness and species deletion stability. In terms of parameters, λ is set to 0.1, and 1.0 is used both as the minimum and initial population size as well as the acceptable threshold for the ecological loop to have reached a stationary state. In all cases, $R = 5 \times 10^4$ in each cell. For the systems of two or three cells, we always set $c = 0.6$ and $b = 0.005$. However, in the four-cell scenarios we consider two different schemes: uniform-(c, b) where in all cells these two parameters are as before, and heterogeneous-(c, b) systems where they vary spatially. In this case, the following values are used: (0.8, 0.001), (0.7, 0.005), (0.6, 0.01), and (0.5, 0.02). We note from our own previous work [AMG19] and that of other authors [QHM05b] that when c is high (0.7, 0.8) it places some limitations on the diversity of the local food web, but the values of the predator saturation constant (b) chosen here should not be limiting. To better understand the effect of coupling cells with these different parameter choices, we then studied two scenarios with spatially-uniform c and b, but choosing the most extreme combinations that were used in the heterogeneous scenarios. That is, these two scenarios respectively take the (c, b) parameter sets (0.8, 0.001) and (0.5, 0.02) for all cells.

We perform five simulations for each scenario, except for scenario 11, which requires ~ 2 months per simulation on a Skylake i7 processor. We therefore collected just two simulations for this scenario.

3.1. Scenarios

For systems of either two or three cells, we divide scenarios according to the nature of the resources. Either each cell (each local site) has a unique resource, or else they all share the same resource species and are in this way spatially homogeneous. Furthermore, we investigate both the cases where the resource population or biomass is static as in previous research, or where it is time-varying in the ecological loop.

For two-cell systems, each simulation consists of 200 000 evolutionary timesteps, with migration permitted between the 80 000th and 160 000th. For simulations with three cells, arranged in a line with the middle cell adjacent and connected to both others, migration is activated from the 100 000 to 200 000th of the 300 000 evolutionary timesteps. Since each evolutionary timestep represents one speciation event for a local population in one cell of the metacommunity, we perform simulations of a length equal to 100 000 per cell, so that the results are comparable to a regular single-cell simulation of length 100 000 timesteps. For both two- and three-cell scenarios, stability measures of robustness and species deletion stability are recorded every 5000 evolutionary timesteps. All other properties are recorded at intervals of every 10 evolutionary timesteps. The remaining ten

Scenario No.	Number of Cells	Resource Species	Resource Population
1		Homogeneous	Static
2	2	Homogeneous	Time-varying
3		Heterogeneous	Static
4		Heterogeneous	Time-varying
5		Homogeneous	Static
6	3	Homogeneous	Time-varying
7		Heterogeneous	Static
8		Heterogeneous	Time-varying

Table 1: Two and Three Cell Scenarios

scenarios are of systems with four cells. For each of these, there is a unique resource in each cell with static population. Instead

we consider the effects of two other modelling choices: firstly, the spatial topology of the metacommunity. We consider four choices: ring (where the first and fourth cells are connected to both the second and third, but not to each other, and the second and third cells are not directly linked), fully-connected, star (where all cells are connected only to the first cell), and line where the first cell is connected to the second, the second to both the first and third, the third to both the second and fourth, and the fourth cell is connected only to the third. Second, whilst all of these scenarios are spatially heterogeneous in the sense that different resource species are present in each cell, as discussed in the preceding section we also consider, for each topology, the possibility of heterogeneity in the parameters b and c. In all cases, the simulations are performed for 400 000 evolutionary timesteps, with migration occurring between the 100 000 and 300 000th. Given the already high computational demand of these simulations, for scenarios 9-16 we limit the stability properties to be collected only every 10 000 evolutionary timesteps. For the final two scenarios robustness data was not collected, as we are primarily concerned with the effect of the parameter choices on global diversity in these cases.

Scenario No.	Number of Cells	Spatial Topology	(c, b) parameters
9	4	Ring	Homogeneous
10	4		Heterogeneous
11	4	Fully-connected	Homogeneous
12	4		Heterogeneous
13	4	Star	Homogeneous
14	4		Heterogeneous
15	4	Line	Homogeneous
16	4		Heterogeneous
17	4	Line	Homogeneous: high b, low c
18	4		Homogeneous: low b, high c

Table 2: Four Cell Scenarios

Comprehensive experimental data including evolutionary time-series of every property collected, and snapshots of the food webs in each cell during the simulation, pertaining to each simulation conducted (five for all scenarios except for scenario 11 which has only two simulations) can be found in the online supplementary material which accompanies this article. However, for this article we shall present only selected observations of the behaviour for each scenario over multiple simulations, mainly pertaining to the diversity and the degree of similarity between the local networks.

3.2. Averaged data: effect of migration

For the 18 scenarios described, we select several key properties of the food webs: global diversity, average local diversity, the average local link-density, the average local connectance, and the average local maximum and average (over species) shortest-chain trophic levels. We split each simulation into four phases: the period before migration, the period during migration, and then we split the remaining period after migration into two phases of equal duration in terms of evolutionary timesteps. We calculate the mean value of each property under consideration over each of the four phases of the simulation. For each scenario, then we average the values over the respective phases over each simulation for that scenario (two for scenario 11, and five otherwise). The results of this procedure are presented in Figures 1-6, with sets of scenarios with similar properties (e.g. three cells) grouped together.

In particular, Figure 1 shows the global diversity (the total number of unique species alive in the metacommunity) averaged over each of the four phases of all the simulations for each scenario. The results for the scenarios are grouped according to the number of cells (Figure 1(a) illustrates scenarios 1-4 featuring two cells, while Figure 2(b) shows the results for scenarios 5-8 featuring three cells), and, for four cells, the (c, b) parameters. Thus Figure 1(c) displays the results gathered for spatially-homogeneous (c, b) parameters (scenarios 9, 11, 13 and 15) while Figure 1(d) shows those for scenarios with heterogenous (c, b) environments (scenarios 10, 12, 14 and 16). Finally, Figure 1(e) illustrates the global diversity results for scenarios 17 and 18 which featured spatially-homogeneous but extreme choices of c and b. The remaining five properties of interest are presented similarly in Figures 2-6. The prey-averaged tropic levels were considered, but found to follow a similar pattern to the shortest-chain trophic levels.

Two additional properties are presented in tables. We calculate the average total evolutionary lifespans of all species throughout each simulation, and provide the mean of this value for each scenario in Tables 3 and 4. Finally, to help us study the degree of synchronisation between local food webs during the period of migration, we calculate a "synchronisation ratio" by the ratio of the local average number of non-resource species to the global number of non-resource species during the migration period of the simulations for each scenario. This quantity (shown in Tables 5 and 6) is more useful to measure diversity between networks in the metacommunity than the fractions of unique and shared species (time series of which are shown in the supplementary material), as for example in the four-cell systems it could be the case that two cells completely contain half of the set of species while the other two cells contain the other half. This would result in all cells having 100% "shared" species, not revealing that two completely distinct ecosystems have emerged.

	Two Cells				Three Cells			
Scenario	1	2	3	4	5	6	7	8
Lifespan	545.9	645.7	280.3	272.6	419.9	469.2	274.6	357.2

Table 3: Average Evolutionary Lifespans: Two and Three Cell Scenarios

	Four Cells									
Scenario	9	10	11	12	13	14	15	16	17	18
Lifespan	412.1	57.7	326.2	58.5	509.6	86.9	442.5	74.6	26.7	859.7

Table 4: Average Evolutionary Lifespans: Four Cell Scenarios

	Two Cells				Three Cells			
Scenario	1	2	3	4	5	6	7	8
Sync. Ratio	0.692	0.679	0.833	0.843	0.541	0.537	0.654	0.674

Table 5: Average Synchronisation During Migration Period: Two and Three Cell Scenarios

	Four Cells									
Scenario	9	10	11	12	13	14	15	16	17	18
Sync. Ratio	0.681	0.771	0.852	0.853	0.511	0.569	0.526	0.595	0.691	0.490

Table 6: Average Synchronisation During Migration Period: Four Cell Scenarios

(a) Two Cells

(b) Three Cells

(c) Four Cells - Homogeneous (c, b)

(d) Four Cells - Heterogeneous (c, b)

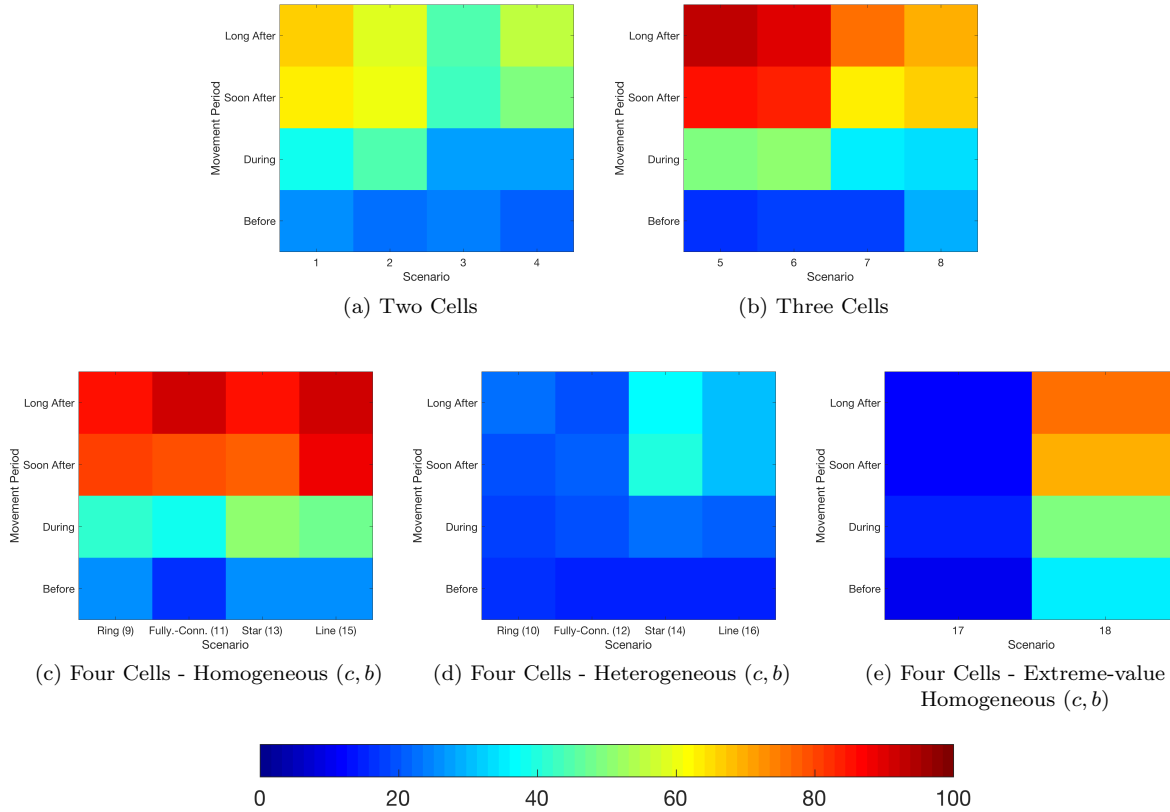(e) Four Cells - Extreme-value Homogeneous (c, b)

Figure 1: Global Diversity

3.3. Observations

For most of the 18 scenarios, all five simulations appear qualitatively similar to each other in their trends and general behaviour (for the time-series of many properties for each simulation, refer to the supplement). The food webs experience

(a) Two Cells

(b) Three Cells

(c) Four Cells - Homogeneous (c, b)

(d) Four Cells - Heterogeneous (c, b)

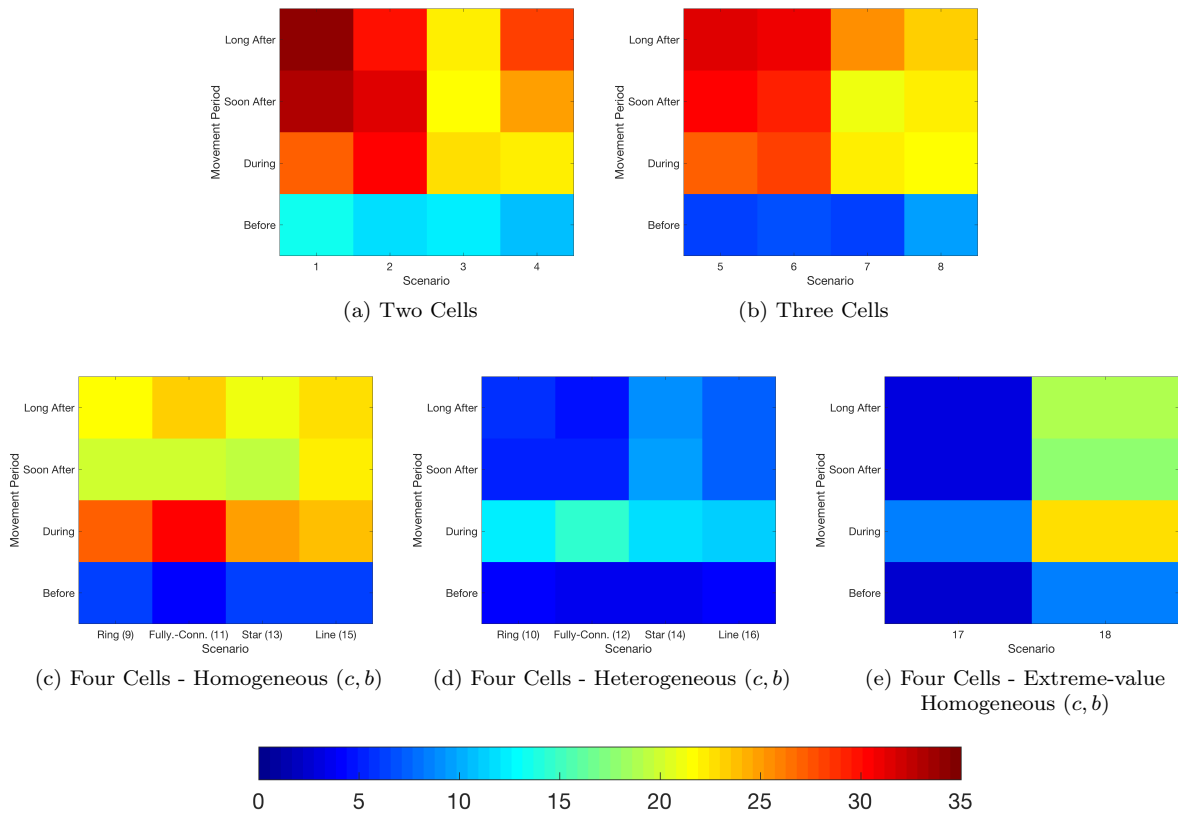(e) Four Cells - Extreme-value Homogeneous (c, b)

Figure 2: Average Local Diversity

growth in global diversity across all four stages of the simulation (Figure 1), albeit at different rates. Visual inspection reveals that varying the population of the resources in the ecological loop has little effect over the range of frequency and amplitude we considered (Figure 1-6(a),(b)).

We observe one major benefit of enabling migration between cells - at least for temporary periods. Simulations of the Webworld model usually have an initial transient period of "pre-complexity" during which the system is unstable and diversity rapidly rises and falls. Some cells may even go extinct altogether in the first few evolutionary timesteps. These experiments demonstrate that when migration is switched on, the networks in any cells which have not yet attained complexity will do so extremely rapidly. There is not even a requirement to couple underdeveloped cells with a sufficiently complex network, as coupling three small food webs immediately results in complexity (e.g. supplement, Figure 1.101). Other properties are strongly influenced by this. Once all of the local webs have left their "pre-complexity" stage, link density is typically between 2 and 3. Connectance typically takes a value between 0.2 and 0.3 when the webs have stabilised (Figure 4). As it is large when networks are small, in most cases it decreases when migration is enabled and then remains low.

Comparing the systems of two and three cells, they display very similar trends. There is a clear distinction between systems with spatially-homogeneous (Scenarios 1,2,5,6) and heterogenous (Scenarios 3,4,7,8) resource species. In simulations where all cells have the same resource species, enabling dispersal has much greater benefits to both global and local diversity, although local diversity nonetheless rises again slightly after movement is turned off (Figure 1-6(a),(b) left-hand columns). Switching on movement between cells with distinct resources also sees an overall increase in both local and global diversity (and the benefit of kickstarting dead or pre-complexity ensembles still applies), but the effect is significantly reduced (Figure 1-6(a),(b) right-hand columns). After movement is disabled, these systems undergo a brief period of fluctuation, as immigrant populations that are not well-adapted to the now-isolated local environment go extinct, before seeing much greater increases in diversity as each cell is free to pursue species that are well-adapted to it. The average evolutionary lifespans of species also tend to increase in such systems after migration has been disabled (Table 3).

In research conducted with a spatial extension of the Loeuille-Loreau model, simulations with heterogeneous environments and diffusive migration nonetheless resulted in identical networks [AWRD15]. Examining the time-series (refer to supplement) reveals that this is also the case in our simulations, with the cells in heterogenous-scenarios possessing few unique species during migration. Curiously, the scenarios with homogenous resources feature about as many unique as shared species in each cell during the period of migration, which is the cause of the greater global diversity, and Table 5 confirms that these scenarios
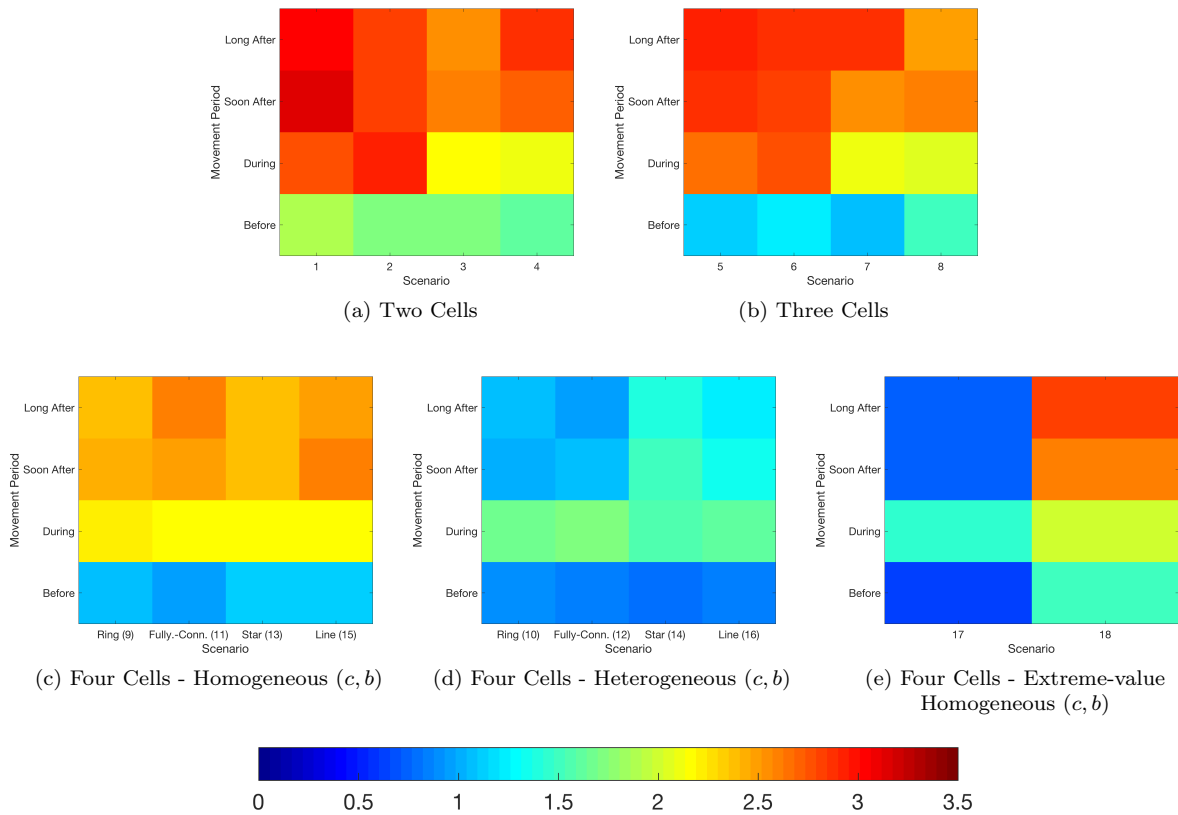
(a) Two Cells   (b) Three Cells

(c) Four Cells - Homogeneous (c, b) (d) Four Cells - Heterogeneous (c, b) (e) Four Cells - Extreme-value Homogeneous (c, b)

Figure 3: Average Link Density

have lower synchronsiation ratios that those with spatially-distinct resources. So coupling sites with completely identical local conditions by a moderate rate of diffusion migration results in distinct networks if the local networks are allowed to evolve before migration begins. It is likely that each cell already hosts some species that are well-adapted to local conditions. In our previous paper, we determined that simulations of Webworld with the same resource would tend to result in some of the same traits [AMG19]. Therefore when migration begins, invaders with low populations are facing competition from entrenched and similar competitors, and cells retain some of their unique particular species. This contrasts with the heterogeneous case, where the immigration of completely different species is much more disruptive, creating an opening for more globally-dominant species to arise and thus resulting in a greater degree of synchronisation between networks.

When the same resource is shared across multiple cells, species which are in common across these cells tend to occupy lower trophic levels than those species which are unique to a given cell. This is because lower level species possess larger populations and this facilitates diffusion migration. The effect of migration on the rate of successful invasions for species at greater than trophic level 1, or non-basal species, also depends on this factor: With the same resource, this rate decreases during migration and then rises when it is switched off, while in systems with different resources the reverse pattern is observed. The trends for maximum and average local SCTL parallel local diversity (Figure 5-6): in all cases, these properties increase during migration, and then for many scenarios (particularly those with heterogeneous resources) there is then a decrease after migration ends.

Next we study the patterns observable for four-cell scenarios. In all these cases, the systems feature a unique resource species in each cell and local diversity temporarily decreases when migration is disabled. This reduction in local diversity did not always occur for systems of two or three cells, so its consistent occurence in four-cell systems may be because a trend discussed previously is exacerbated: for all the four-cell scenarios, there are distinct resource species in each cell. Previously we noted that this could cause fluctuation in local diversity when population movement was switched off. In the four-cell case the system will take longer (in terms of evolutionary timesteps) to recover from this dip due to the increased number of cells, which may result in the dip being significant and lasting for long enough that the local diversity averaged over the third time-period is less than during the period of migration.

Examining Table 6 reveals the role of spatial toplogy in these simulations. As we would expect, local networks in fully-connected metacommunities show a greater degree of synchronisation, while those in scenarios with line and star topologies are the least synchronised. Thus, in addition to the impact of homogeneous or heterogenous resources discussed above, the number of cells and the spatial topology also play a role in determining how diverse the local food webs are during migration.

(a) Two Cells   (b) Three Cells

(c) Four Cells - Homogeneous (c, b) (d) Four Cells - Heterogeneous (c, b) (e) Four Cells - Extreme-value Homogeneous (c, b)
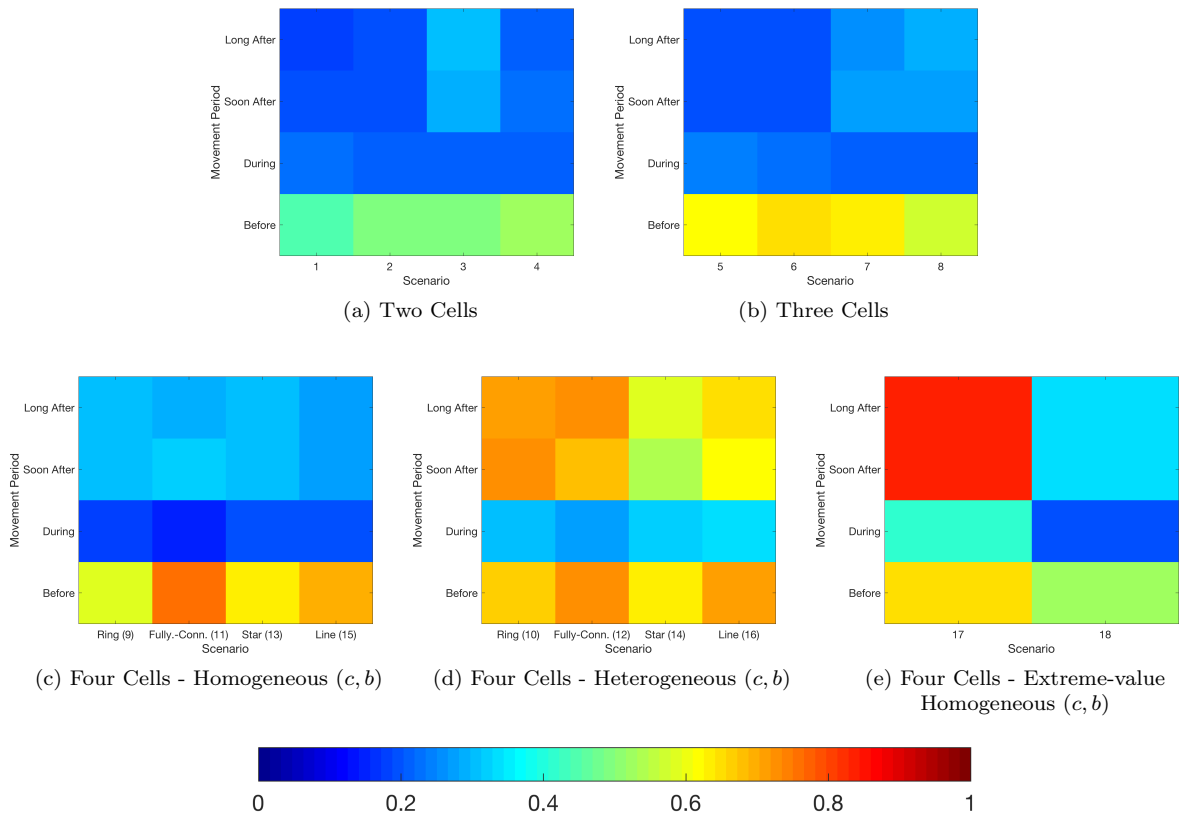
Figure 4: Average Connectance

Overall, choosing homogeneous resources results in significantly reduced synchronisation, but for larger numbers of cells this can also be achieved by less-connected spatial topologies (line, star, and to a lesser extent ring) so that systems of four cells with heterogenous resources can still maintain some distinctness between cells when using the moderate diffusion rate employed in these simulations. As we shall see later in Section 5, when the diffusion rate is greater and there are fewer cells, heterogeneous resource systems will become fully-synchronised.

We also note that for four-cell systems both the average and maximum SCTL decrease in all cases when migration is disabled. Since we already know that shared species tend to occupy lower trophic levels, this decrease is probably due to the local food webs shrinking as they try to rebuild themselves with an optimal local arrangement that suits the local resource species, rather than it being the case of higher level species being maintained by migration and then lost when it is switched off. The effect is also observed for two and three-cell systems with heterogeneous resource species.

Let us consider the role of the (c, b) environmental parameters. Unlike the choice of resource species, this involves coupling food webs that may be constrained to fundamentally different network structures when these parameters are spatially-variable. Compared to the homogeneous (c, b) scenarios (Figure 1-2(c)), it is very clear that the heterogeneous (c, b) scenarios result in greatly reduced global and local diversity across all topologies and time-periods after migration has begun (Figure 1-2(d)), and the food webs are thus generally more synchronised (Table 6). Such systems show greater variation in most properties during and after migration relative to their uniform (c, b) counterparts, and the post-migration decrease in maximum and average shortest-chain trophic levels is particularly evident (Figure 5-6(d)). Their species have lower average evolutionary lifespans (50-70 evolutionary timesteps) than the uniform (c, b) systems (300-500) (Table 4). Species lifespans tend to increase when migration is enabled in homogeneous environments, but for heterogeneous (c, b) environments they may decrease during migration and then rise again after it is disabled. In heterogeneous (c, b) environments species turnover and the likelihood of successful invasion increase significantly when migration is switched off. Amongst these systems, the lack of equilibrium is even more pronounced with line topology (scenario 16), probably because the most stable cell struggles to damp out the destabilising effect of the least stable, whilst star topology (scenario 14) results in the greatest local diversity (Figure 2(d)).

In order to further investigate the role of parameter heterogeneity, we consider scenarios 17 and 18. We find that the systems with low b and high c (scenario 18) operate normally, with rapid growth followed by a very significant decrease in diversity in some cells (Figure 2(e)), but not globally (Figure 1(e)), when migration is switched off. However, for scenario 17 (high b and low c) the network's properties appear very similar to those of the heterogeneous systems, with low diversity in all cells, and

(a) Two Cells

(b) Three Cells

(c) Four Cells - Homogeneous (c, b)

(d) Four Cells - Heterogeneous (c, b)

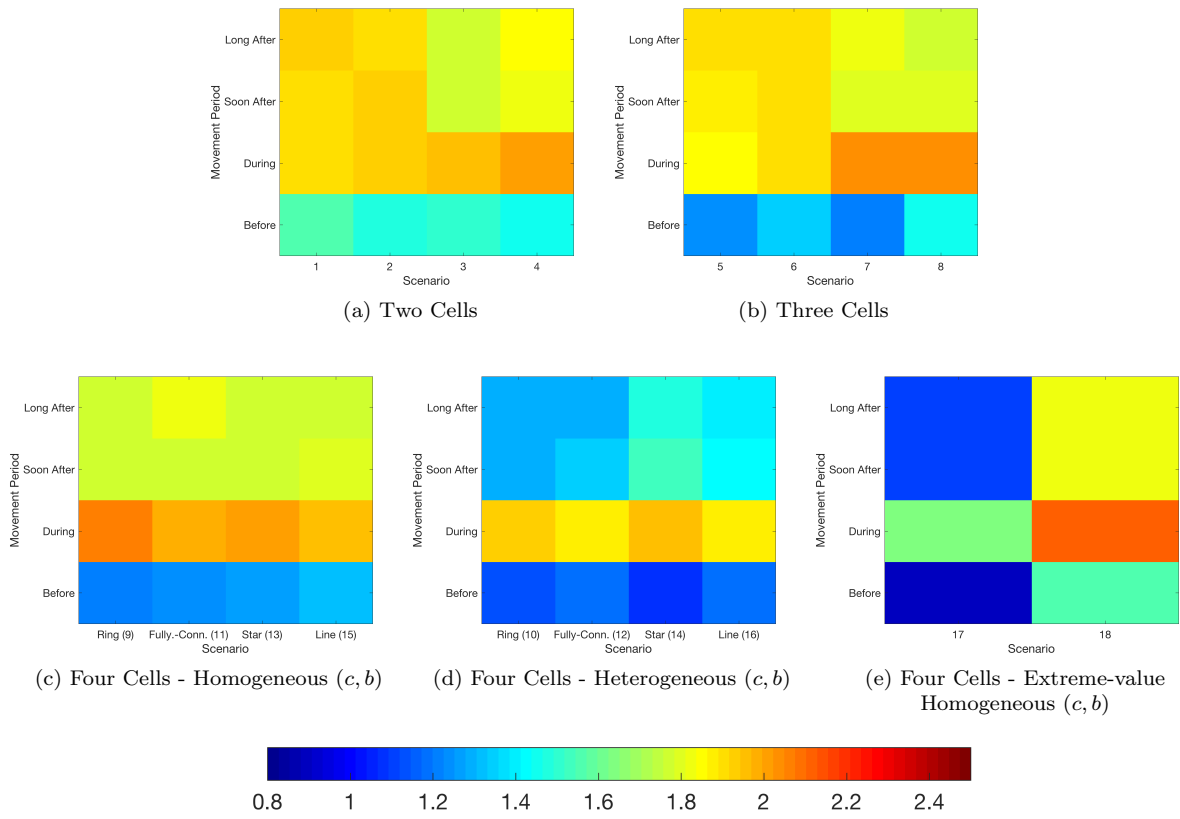(e) Four Cells - Extreme-value Homogeneous (c, b)

Figure 5: Average Shortest-chain Trophic Level

with constant fluctuation in all properties over time. Evolutionary lifespans are even more reduced (from approximately 50-80 to between 25 and 30 evolutionary timesteps) compared to the heterogeneous (c, b) scenarios, and the phylogenetic trees of the surviving species' ancestry indicate that very few species endure for many evolutionary timesteps, quite distinct from any other scenario investigated in this experiment. Clearly, the cell with these (c, b) values in the heterogeneous scenario had a strongly destabilising effect on metacommunity, and so these negative effects were not entirely due to heterogeneity itself.
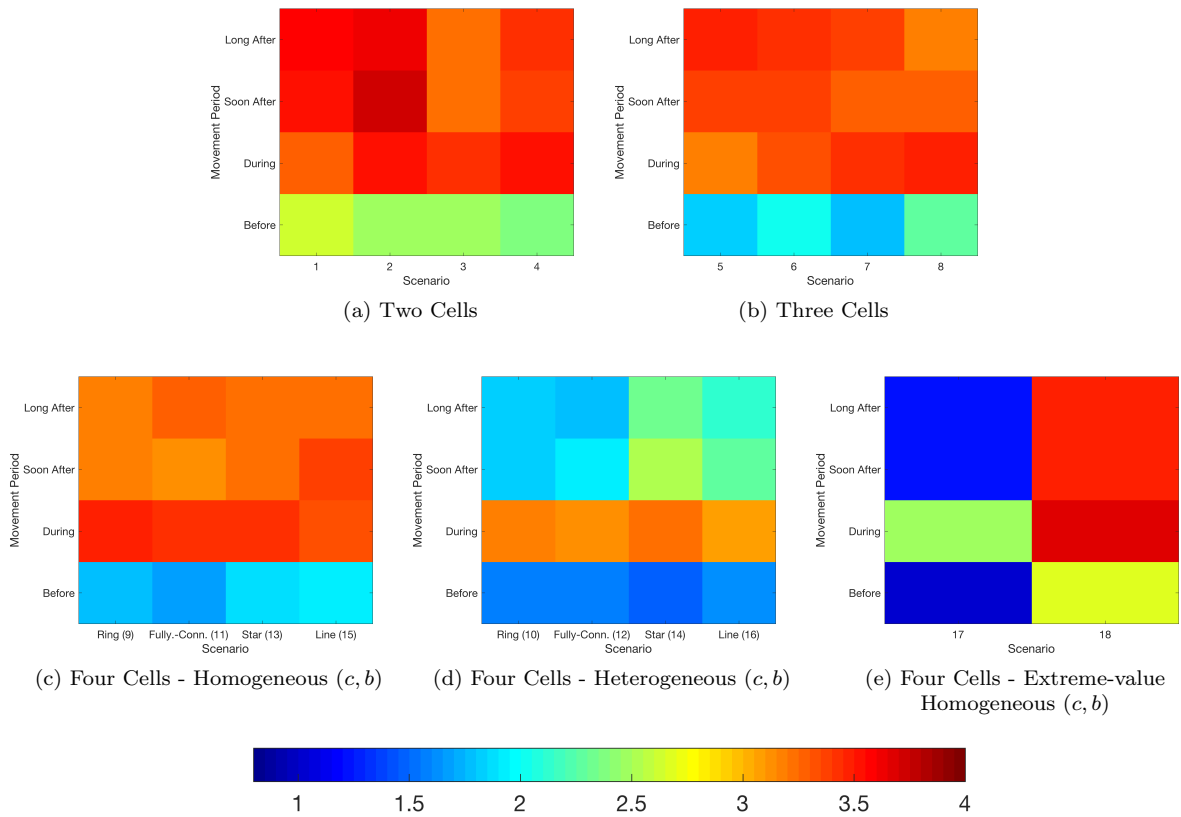
Figure 6: Maximum Shortest-chain Trophic Level

4. The role of resource size on global and local properties

Consider a four-cell ring metacommunity, with $c = 0.6$ and $b = 0.005$ in each cell (i.e. uniform (c, b)) and a unique resource species in each environment. We investigate the influence of the resource biomass (uniform across all cells) on the local and global properties of the food webs. Each simulation is performed for 300 000 evolutionary timesteps, with constant diffusion migration permitted from the 100 000th evolutionary timestep until the end of the simulation, occuring at a rate of 0.005 of each population moving along each of the two links out of each cell to its neighbours at every ecological timestep.

We see that global diversity is substantially greater than average local diversity in this experiment (Figure 7), similar to the corresponding scenario 9 in Section 3 (four-cells in a ring with uniform (c, b) and heterogeneous resource species). In particular, the moderate rate of diffusion results in a ratio of local to global diversity of approximately $2/3$ as we would expect (scenario 9, Table 6). The local food webs are even more distinct from each other when the resource is low, as there are fewer species and lower populations supported, so it is less likely that a species well-adapted to cell (1,1) will be able to migrate and establish a satellite subpopulation in cell (2,2). This diminishing growth of diversity with resource size is in broad agreement with previous results for the original, non-spatial version of the model [McK04].

In line with our previous experiments [AMG19], the average L/S in each cell increases slowly and local connectance declines to between 0.1 and 0.2 as the diversity increases along with the resource biomass. We find that measures of trophic height and trophic level return very similar results, and both the average and maximum values of these in the system are saturating to about 2.4 and 4.4 respectively as the resource increases (not shown).
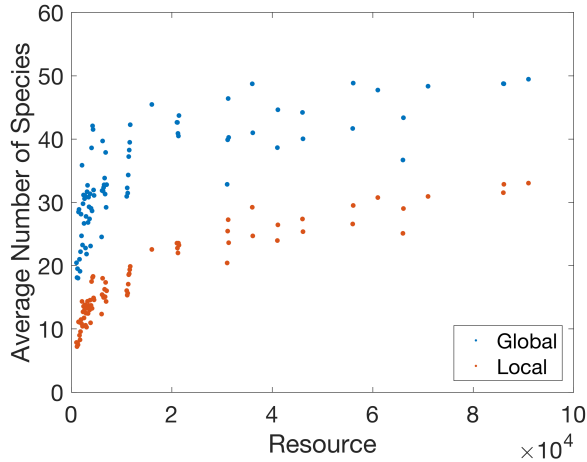
(a) Diversity

Figure 7: Effect of Resource

5. Effect of migration implementation and rate

We investigate the impact of the frequency and the magnitude of dispersal events for a variety of migration schemes in systems of three cells that are arranged in a line. That is, one cell is connected to both of the others, but these two are not directly connected to each other. For the first two schemes, we also performed similar tests with a fully-connected metacommunity, but like other authors ([TD18]) found that the impact of this topology is negligible.

In particular, we consider the average local diversity (the number of species actually present with population greater than 1.0 in the cell at that time), the global diversity (total number of unique species in the system), and the average of the following properties over all three cells in the metacommunity: link density, connectance, average and maximum shortest-chain trophic levels in the cell. The prey-averaged trophic levels were also calculated and found to follow a near-identical pattern to the shortest-chain trophic levels in all cases.

For all of these experiments, each cell has the parameters $c = 0.6$, $R = 1 \times 10^4$. As usual, $\lambda = 0.1$ and $b = 0.005$. For 100 values of the migration constant $\phi = 1, 2, \ldots, 100$, the system is iterated for 300 000 evolutionary timesteps, with migration beginning at the 100 000th and continuing until the end of the simulation. Each graph is therefore the result of 30 000 000 speciation events. Results are averaged over the final 10 000 timesteps, during which migration is still permitted.

In our other work on this model [AMG19], a single isolated food web with the same parameters could average between 27 and 32 unique species. Performing 50 simulations with three disconnected cells for 300 000 evolutionary timesteps, which differs from simulating a single cell in the effect of the probabilistic parental-selection mechanism and tripling the energy input via three resources each with $R = 10^4$, yielded the following results: global diversity 45.34 averaged over the final 10 000 evolutionary timesteps, and (also averaged over all of the cells) local diversity 16.99, link density 2.10, connectance 0.40, maximum and average shortest chain trophic levels 2.45 and 1.46, and average and maximum prey-averaged trophic levels 2.61 and 1.52. These experiments lack the benefits of a regular spatial simulation which feature periods of movement, and combined with the effect of the speciation mechanism for multiple disconnected cells this results in a large degree of variation in diversity between cells and between simulations - much more so than we have previously seen from the Webworld model, which for a single cell is relatively consistent provided that the number of evolutionary timesteps is sufficiently large. Furthermore, individual cells were allowed to collapse, further reducing the average local diversity relative to the equivalent single-cell simulations despite the increased total resources. In the plots for this section, the corresponding values for this control set with no migration are indicated by dashed lines.

5.1. Diffusion

As in the results presented in the previous section, we first assume that species migrate between adjacent cells by density-dependent diffusion so that if a given cell is connected to k other cells, then a fixed fraction $\rho = \phi/100$ of the populations of each non-resource species in that cell will move to each of the k other cells. In other words, there is a uniform fraction of movement along each link, but not a uniformity in the fraction of populations leaving each cell unless all cells have an equal degree of connectivity. If more than the entire population of a species is to leave a cell, that is if $k\rho > 1$, then the migrating populations are normalised and $\frac{1}{k}$ moves to each connected cell. More general to that used in the previous sections, the movement function

μ for the amount of species i which moves from cell (j,k) to cell (x,y), is given by:

$$\mu_{i,j,k,x,y} = \frac{\phi}{100} \times N_{i,t}^{j,k} \tag{6}$$

5.2. Adaptive migration

For a different scheme, we studied the outcome of populations only moving as a result of unfavourable conditions in their current local environment, similar to the adaptive migration schemes used by other authors [AWRD15]. In this case, we record the population of each species in each cell at each ecological timestep. If the local population declines between subsequent timesteps, as a result of the feeding and reproduction (i.e. excluding the effects of migration at the previous timestep), then a fraction of the population will emigrate to each connected cell in proportion to the fraction of decline. This mechanism was chosen as it does not require choosing a relative weighting between seeking to find abundant prey, avoiding predators, and desiring better environmental conditions. All of these factors are implicitly taken into account by measuring their actual outcome on local populations. In particular, for a cell of degree k, $\rho \times$ (fractional decrease) will move to each of k other cells, where $\rho = \phi/50$. Thus, ρ scales the rate of movement and how small a population decline is required for saturation of the movement function, where the entire species emigrates. For example, in the middle cell with degree 2, the entire local population will abandon the cell if it declines by a fraction of at least $1/2\rho = 50/2\phi = 25/\phi$. The movement function for species i at ecological timestep $t > 1$ is therefore:

$$\mu_{i,j,k,x,y} = \frac{\phi}{50} \times \max\left(0, \frac{N_{i,t-1}^{j,k} - N_{i,t}^{j,k}}{N_{i,t-1}^{j,k}}\right) \tag{7}$$

5.3. Diffusion version 2 (V2)

Next, we implement a slightly different version of diffusion where local populations migrate to adjacent cells by density-dependent diffusion so that if a given cell is connected to k other cells, then some fixed fraction $\rho = \phi/100$ of the populations of each non-resource species in that cell will emigrate, evenly split between the k neighbours (i.e. the level of emigration will be independent of the degree of the cell). Therefore in this case the migration parameter ϕ is just the percentage of each local population that emigrates from every cell at every ecological timestep. The movement function is divided by the degree k, and so we have:

$$\mu_{i,j,k,x,y} = \frac{\phi}{100k} \times N_{i,t}^{j,k} \tag{8}$$

5.4. Adaptive migration version 2 (V2)

Similarly, we adopt a scheme where species move at a rate independent of the spatial topology, and only when under pressure in a local environment. If the local population declines between subsequent timesteps, as a result of the feeding and reproduction, then a fraction of the population will emigrate to each connected cell in proportion to the fraction of decline. In particular, for a cell of degree k, $\rho \times$ (fractional decrease) will emigrate, where $\rho = \phi/50$, and so $\phi/(k \times 50)$ goes to each neighbouring cell. For example, the entire local population of any cell will abandon it, equally divided amongst all nighbouring cells, if it declines by a fraction of at least $1/\rho = 50/\phi$. Similar to before, the movement function is given by:

$$\mu_{i,j,k,x,y} = \frac{\phi}{50k} \times \max\left(0, \frac{N_{i,t-1}^{j,k} - N_{i,t}^{j,k}}{N_{i,t-1}^{j,k}}\right) \tag{9}$$

5.5. Stochastic-absolute migration

Next we consider three possible movement schemes to model situations where migration occurs only occasionally, rather than during every ecological timestep. For this, we follow Thiel and Drossel in their investigation using the Niche Model [TD18] and switch to a stochastic implementation. We look at three different ways to scale movement with ϕ from $1, \ldots, 100$: (a) the frequency of the movements increases, (b) the size of movement events increases, and finally (c) both the size and frequency of events increases. In all cases (a)-(c), the rate and degree of movement are independent of any properties of the particular species.

For each cell and local population, and at each ecological timestep, θ is a uniformly-distributed random variable in [0,1). In each case, movement out of the central more-connected cell is doubled in size, but halved in frequency.

(a) For the central cell, migration occurs if $\theta < \phi/2000$, whilst for populations in other cells it occurs if $\theta < \phi/1000$. In all cases, a population size (*not* fraction) of 2.0 emigrates to each connected cell. Therefore, the biomass of species i that moves between (j,k) and (x,y) when connected is given by:

$$\mu_{i,j,k,x,y} = \chi_{j,k,\theta} \times 2.0 \tag{10}$$

where $\chi_{j,k,\theta} = 1$ if $\theta < \phi/2000$ and $j = 2$, or if $\theta < \phi/1000$ and $j \neq 2$, and zero otherwise.

(b) For the central cell, migration occurs if $\theta < 1/2000$, whilst for populations in other cells it occurs if $\theta < 1/1000$. In all cases, a population size of $1.0 \times \phi$ emigrates. Therefore, the movement function is given by:

$$\mu_{i,j,k,x,y} = \chi_{j,k,\theta} \times \phi \tag{11}$$

where $\chi_{j,k,\theta} = 1$ if $\theta < 1/2000$ and $j = 2$, or if $\theta < 1/1000$ and $j \neq 2$, and zero otherwise.

(c) For the central cell, migration occurs if $\theta < \phi/2000$, whilst for populations in other cells it occurs if $\theta < \phi/1000$, with population size $1.0 \times \phi$ emigrating. In this case, the movement function is:

$$\mu_{i,j,k,x,y} = \chi_{j,k,\theta} \times \phi \tag{12}$$

where $\chi_{j,k,\theta} = 1$ if $\theta < \phi/2000$ and $j = 2$, or if $\theta < \phi/1000$ and $j \neq 2$, and zero otherwise.

In these simulations, species occupying the first trophic level typically have population size 100-1000, while many higher level species are of size 5-50. Therefore for stochastic scheme (a), only the very smallest local populations are in the range 1-2 and could be made extinct locally by emigration. For schemes (b) and (c), occassional total displacement of populations could occur for most values of ϕ, especially for $\phi > 5$. However, as ϕ is never of the order of 1000, it does not become large enough to always necessitate that all populations always move (in which case, any greater values of ϕ would be redundant).

5.6. Stochastic-fractional migration

Finally, we consider 400 simulations consisting of four cross-sections of a stochastic migration scheme where a given fraction of the local population migrates at stochastically-chosen ecological timesteps. The first three cross-sections are of a similar form: 20%, 1%, and 0.1% of local populations respectively migrating with frequency at 100 increments between 1/1000 and 1/10 ecological timesteps. The fourth scheme compares directly with the previous stochastic-absolute schemes, as local populations emigrate from cells with a frequency of 1/1000 ecological timesteps. In this last case we explore the impact of varying the fraction of the local population that emigrates over 100 increments between 1% and 100%.

To make these clear, the population of species i that migrate between connected cells (j,k) and (x,y) at a given ecological timestep for these cross-sections (which shall be referred to as stochastic-fractional 1,2,3,4) are as follows:

$$\mu_{i,j,k,x,y} = \chi_{j,k,\theta} \times 0.2 N_i^{j,k} \tag{13}$$
where $\chi_{j,k,\theta} = 1$ if $\theta < \phi/2000$ and $j = 2, k = 1$, or if $\theta < \phi/1000$ and $j \neq 2$, and zero otherwise.

$$\mu_{i,j,k,x,y} = \chi_{j,k,\theta} \times 0.01 N_i^{j,k} \tag{14}$$
where $\chi_{j,k,\theta} = 1$ if $\theta < \phi/2000$ and $j = 2, k = 1$, or if $\theta < \phi/1000$ and $j \neq 2$, and zero otherwise.

$$\mu_{i,j,k,x,y} = \chi_{j,k,\theta} \times 0.001 N_i^{j,k} \tag{15}$$
where $\chi_{j,k,\theta} = 1$ if $\theta < \phi/2000$ and $j = 2, k = 1$, or if $\theta < \phi/1000$ and $j \neq 2$, and zero otherwise.

$$\mu_{i,j,k,x,y} = \chi_{j,k,\theta} \times 0.01 \phi N_i^{j,k} \tag{16}$$
where $\chi_{j,k,\theta} = 1$ if $\theta < 1/2000$ and $j = 2, k = 1$, or if $\theta < 1/1000$ and $j \neq 2$, and zero otherwise.

5.7. Observations

In Figures 8-11 we see that all properties generally show moderate fluctuation due to small changes in the migration parameter. Both diffusion schemes are particularly affected, while stochastic-absolute migration 2 return the most consistent results.

When using a deterministic diffusion form of movement, there is a slight downward trend of local diversity as a greater fraction of the populations migrates, but it is obscured by the high level of variability with the migration parameter. In contrast, the effect of this degree of mixing on the global diversity is obvious and consistent, reducing it to about the same level as the local diversity as synchronisation occurs and the local food webs become homogenised. For the very smallest values of ϕ it is visible that global diversity is just beginning to pick up beyond local diversity, leading to the more distinct food webs seen in Section 3 when diffusion occured at a more moderate rate.

The two versions of adaptive migration are the most beneficial at both the local and global levels. In both cases, the average local diversity is around 20 species and the global diversity approximates between 60 and 70. This indicates that the local food webs are mostly distinct from each other. That the diversity is well above the control average of 45 in most cases suggests that rescue effects are in play to allow the local webs to benefit from each other without forcing a diversity-reducing synchronisation. This demonstrates how when each species is acting "intelligently" in its own self-interest, the ecosystem as a
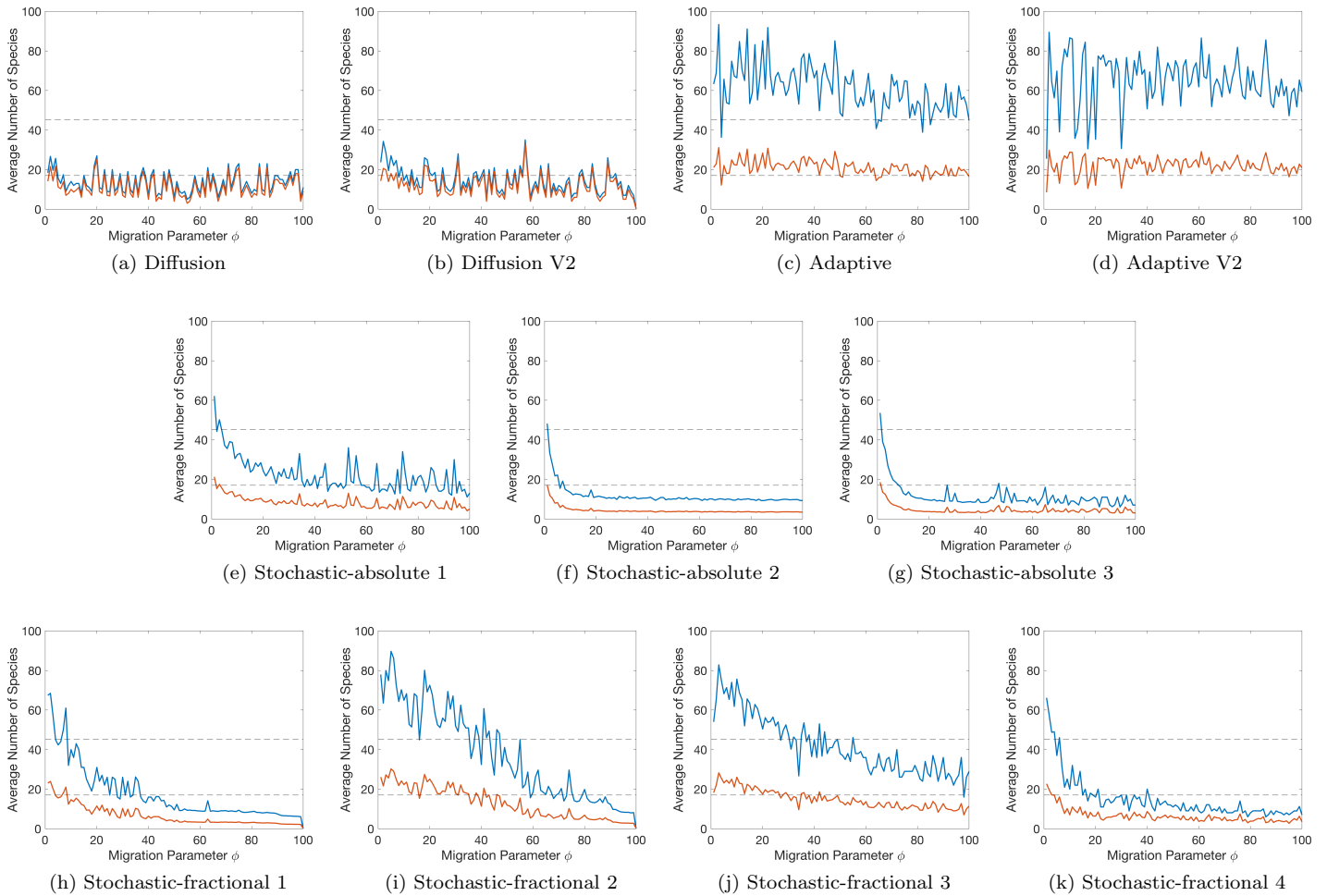
Figure 8: Diversity.
Blue = Global;
Red = Average Local.

whole benefits as more species can be maintained. The exact parameters regarding the magnitude of movement are relatively inconsequential in this scenario.

For all three cases of stochastic-absolute migration, enabling movement that is sufficiently large and frequent has a significantly negative effect on species diversity compared to when no movement is permitted. In particular, for versions 2 and 3, the local food webs in these simulations often had fewer than 10 species once the size of migration events had become sufficiently large. The first stochastic-absolute migration scheme, where the migrating populations are fixed at 2.0 which is small enough to constitute only a minor fraction of most local populations on the first or second trophic levels, shows about the same local diversity as diffusion, but permits greater global diversity (Figure 8(e)) - allowing distinct local food webs to be constructed. Only when the probability of migration is lowest (on the order of one event in every 1000 ecological timesteps per species per cell) does this scheme permit local and global diversity that exceed these properties in the absence of coupling. Similar results are seen with stochastic-fractional migration, where it should occur but as rarely as possible to maximise both local and global diversity. Scheme 4 also indicates (Figure 8(k)) that it is also optimal to have the smallest possible fraction of the local population migrating during an event. Whilst this seems to conflict with scheme 2 (1% movement) reaching greater global diversities than scheme 3 (0.1%), note that as movement becomes more frequent both the local and global diversities decline much more rapidly for scheme 2 than for 3, and so scheme 3 (with its lower amounts of movement) can tolerate more frequent events before reaching lower diversity than the absence of movement.

Comparing diffusion and the stochastic-absolute migration schemes indicates that spatial mechanisms which can occassionally displace large portions of local populations from their environment has a prohibitively negative impact on species diversity at both the local and global levels, whilst schemes which enforce mixing and homogeneity by frequent movement mainly limit global diversity. Stochastic absolute 2 and 3 are actually worse than even high rates of constant diffusion for local diversity, whilst allowing some distinction between the local networks as global diversity is slightly higher than local diversity. Furthermore, the stochastic-absolute schemes demonstrate that some forms of movement actively suppress local diversity compared to isolation,
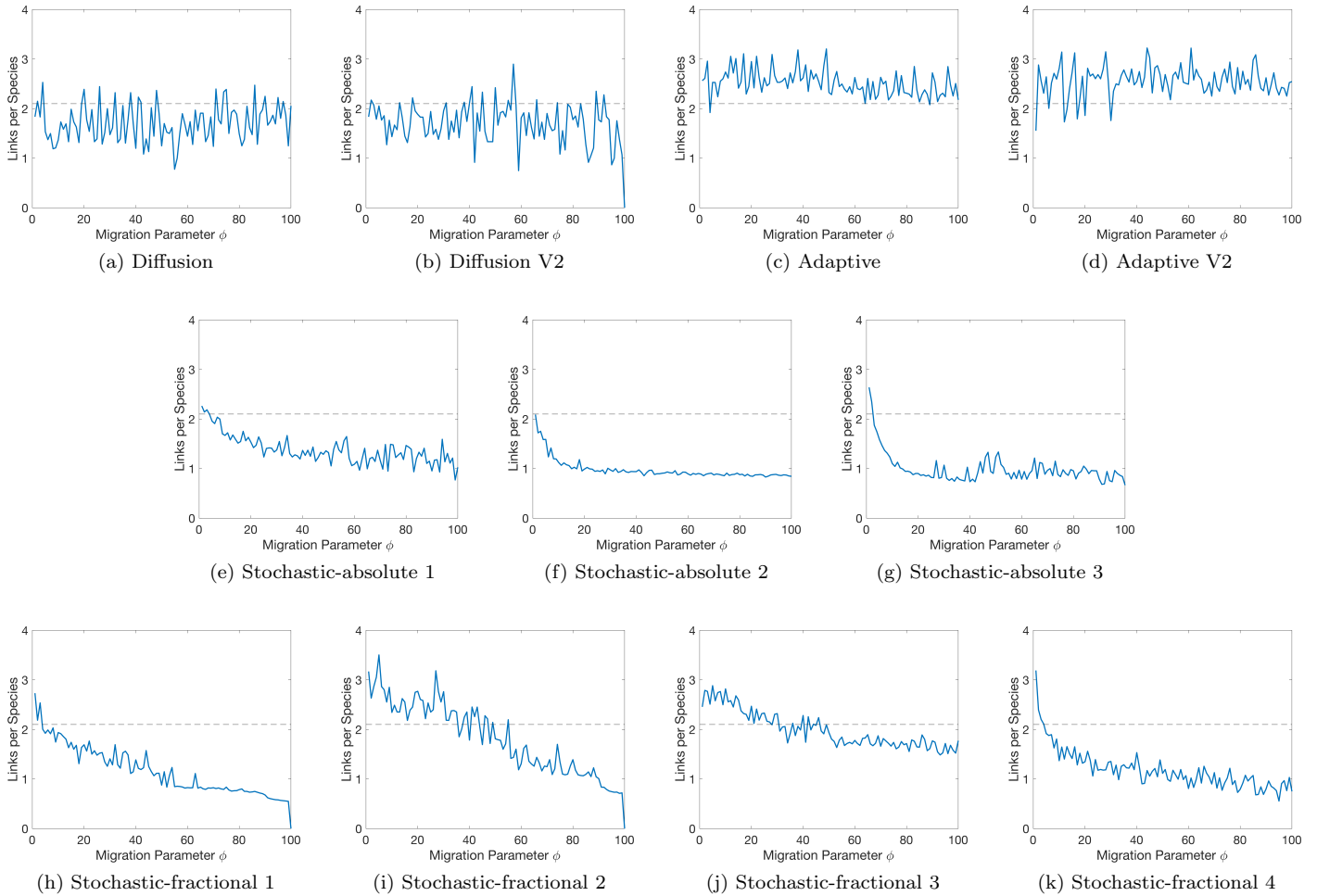
17

Figure 9: Average Local Link Density

whilst studies using other models have concluded that migration generally enhances this property over evolutionary time (e.g. [BDA17]). This is clearly not necessarily the case, and migration can be a negative addition if large populations migrate at low-moderate frequencies (approximately every 1000 ecological timesteps). Overall, implementing migration in a way that allows only tiny fractions of populations to migrate as rarely as possible, or else only in response to unfavourable local conditions, is the most beneficial for species diversity as it can allow for kick-starting diversity in neighbouring cells or providing occasional rescue effects.

We briefly survey the other properties. For diffusion, the average local link density is approximately 2 throughout (Figure 9(a),(b)), and 2.5 for adaptive migration (Figure 9(c),(d)). Connectance remains consistently about 0.2-0.3 for adaptive migration (Figure 10(c),(d)), but for diffusion can rise significantly higher as a consequence of low local diversity for certain values of the migration parameter (Figure 10(a),(b)). For the stochastic migration schemes, as the parameter increases and the local species diversity rapidly drops to very low numbers, consequently the link-density approaches one or less (the resource is counted as a species in this context) and high values of connectance are reached as the webs are reduced to simple food chains with mostly basal and top species. Trends in the measures of trophic level and trophic height for all movement schemes can similarly be explained in terms of the local diversity, with lower values being achieved amongst the kinds of stochastic migration that possess the lowest local diversity. We note that in all cases, prey-averaged measures (not shown) are very close to the shortest-chain variety.

(a) Diffusion   (b) Diffusion V2   (c) Adaptive   (d) Adaptive V2

(e) Stochastic-absolute 1   (f) Stochastic-absolute 2   (g) Stochastic-absolute 3

(h) Stochastic-fractional 1   (i) Stochastic-fractional 2   (j) Stochastic-fractional 3   (k) Stochastic-fractional 4
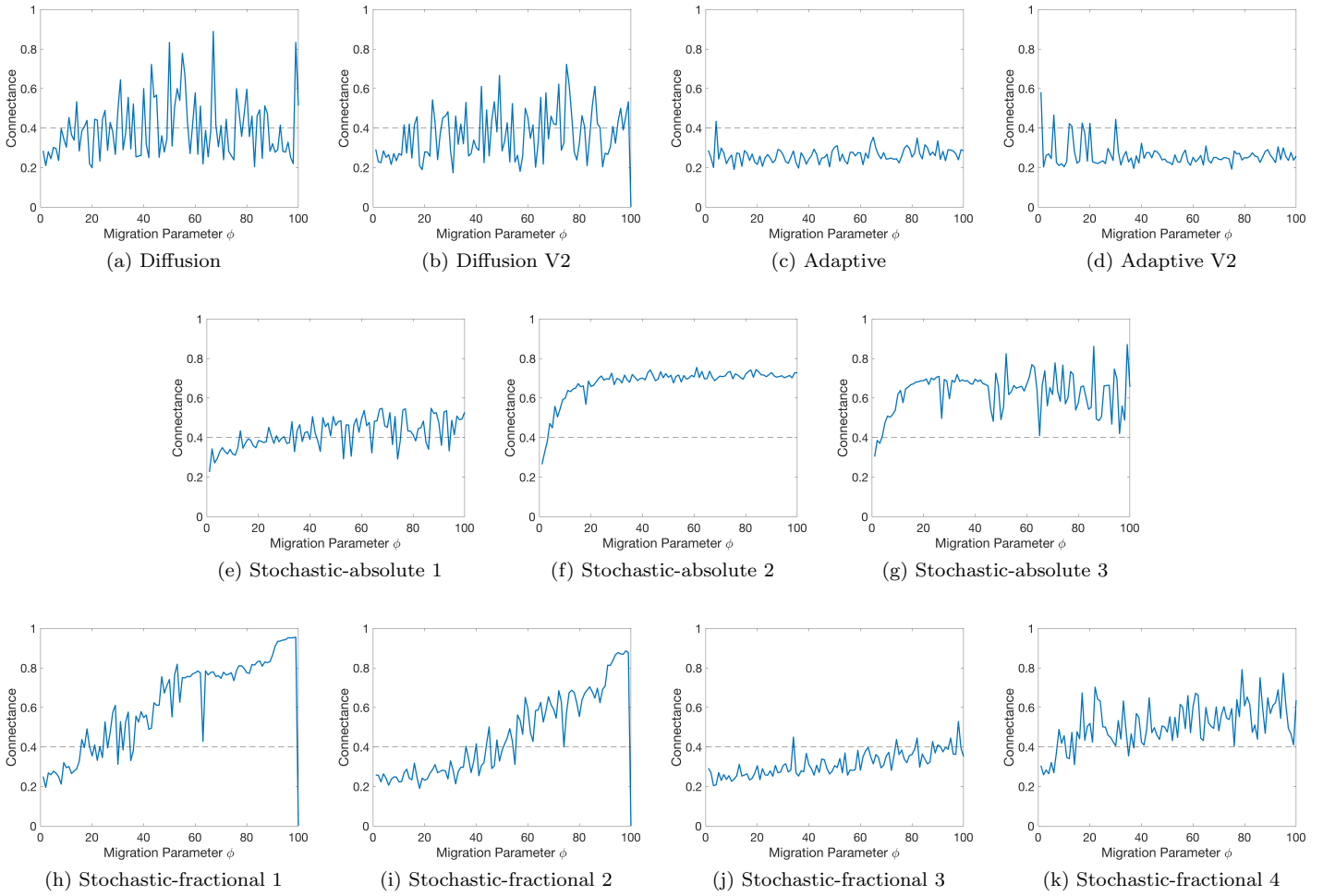
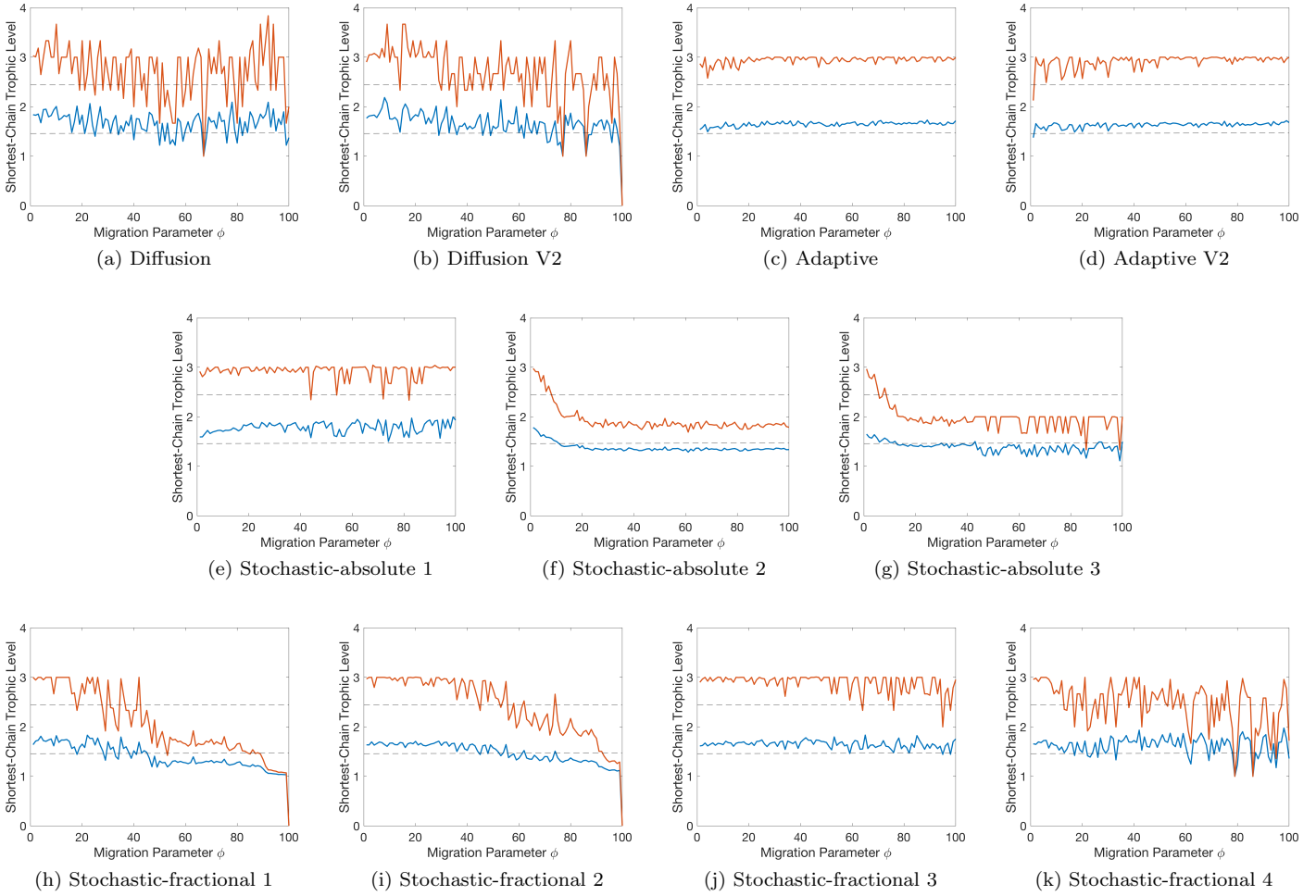Figure 10: Average Local Connectance

Figure 11: Shortest-Chain Trophic Level:
Blue = average of local average SCTL;
Red = average of local maximum SCTL

6. Interaction of stability and migration

In our previous work [AMG19], we studied the stability of the food webs constructed by Webworld using a variety of tools, including robustness and species deletion stability. In Section 3 of this paper, at various points during the metacommunity simulation, we disabled migration and then identified the robustness of the local community that remained in each cell after the effects of isolation had been taken into account. Whilst this yields information about whether exposure to other cells improves the inherent stability of a given cell's local food web, it does not fully account for the effects of ongoing spatial coupling on the ability of a local community to resist and respond to perturbation. To better investigate the interplay of migration and local stability, we created some new measures. First, we disable migration and count the fraction of the non-resource local populations that go extinct during one evolutionary timestep without speciation (i.e. iterating the population dynamics to a steady state) as a result of isolating the cell. During our preliminary tests, we found that sometimes performing a second consecutive iteration of the population dynamics causes additional extinctions during periods where migration was not permitted. To address this, we reduced the tolerance of the population dynamics in this experiment from 1.0 to 0.01 as they search for fixed points or cycles. Next, we calculate both the Robustness and the species deletion stability (the fraction of the non-resource species that can be individually deleted without incurring any secondary extinctions) of the isolated webs, alongside the average number of secondary extinctions that occur when a single species is deleted and the population dynamics subsequently iterated. The latter is averaged over all species deletion tests, including those that result in zero secondary extinctions.

We also introduce two new measures, "dynamic local robustness" and "dynamic global robustness". To determine these values for each of the cells, we randomly choose a non-resource species that is present in the cell, and delete it either just from the cell under consideration, or from the entire metacommunity, respectively *without* first uncoupling the cell during periods of migration. The corresponding robustness value is then the fraction of the number of species present in the cell that must be deleted manually in order to achieve at least 50% of species extinctions from the cell. These experiments are performed 100 times, and the robustness measure is averaged over those experiments for which at least 50% extinction was achieved. We count separately the fraction of experiments for which it is never achieved. To understand why this may be the case during periods of migration, consider an example: Cell A contains n non-resource species, and is coupled to Cell B which maintains large populations of the same set of species. We therefore perform up to n deletions of the local or global populations of randomly selected species present in Cell A. If at a given time after deleting m species in Cell A, $n/2$ or fewer local populations are present, then the robustness is counted as m/n. However, if after every deletion, the local population is replenished (or a new species enters) by immigration from Cell B, then we could perform up to n deletions without the local diversity ever dropping below $n/2$. In such a case, robustness is not recorded, and this experiment is instead counted in the "fraction of surviving experiments".

In particular, we perform two simulations. Each has three cells arranged in a line, with $R = 5 \times 10^4$ and $c = 0.6$ in each cell. The simulations last for 300 000 evolutionary timesteps, with migration permitted between 100 000 and 200 000. Stability properties are calculated every 500 timesteps, and regular properties every 20 timesteps. The first experiment utilises the diffusion V2 migration scheme with rate 0.005, and the second employs the adaptive migration V2 scheme with $\phi = 25$, which means that if a local population in any cell decreases by fraction p between two subsequent ecological timesteps, then a fraction $p/2$ of the remaining population will emigrate at the next timestep, equally divided between them when there are two adjacent cells.
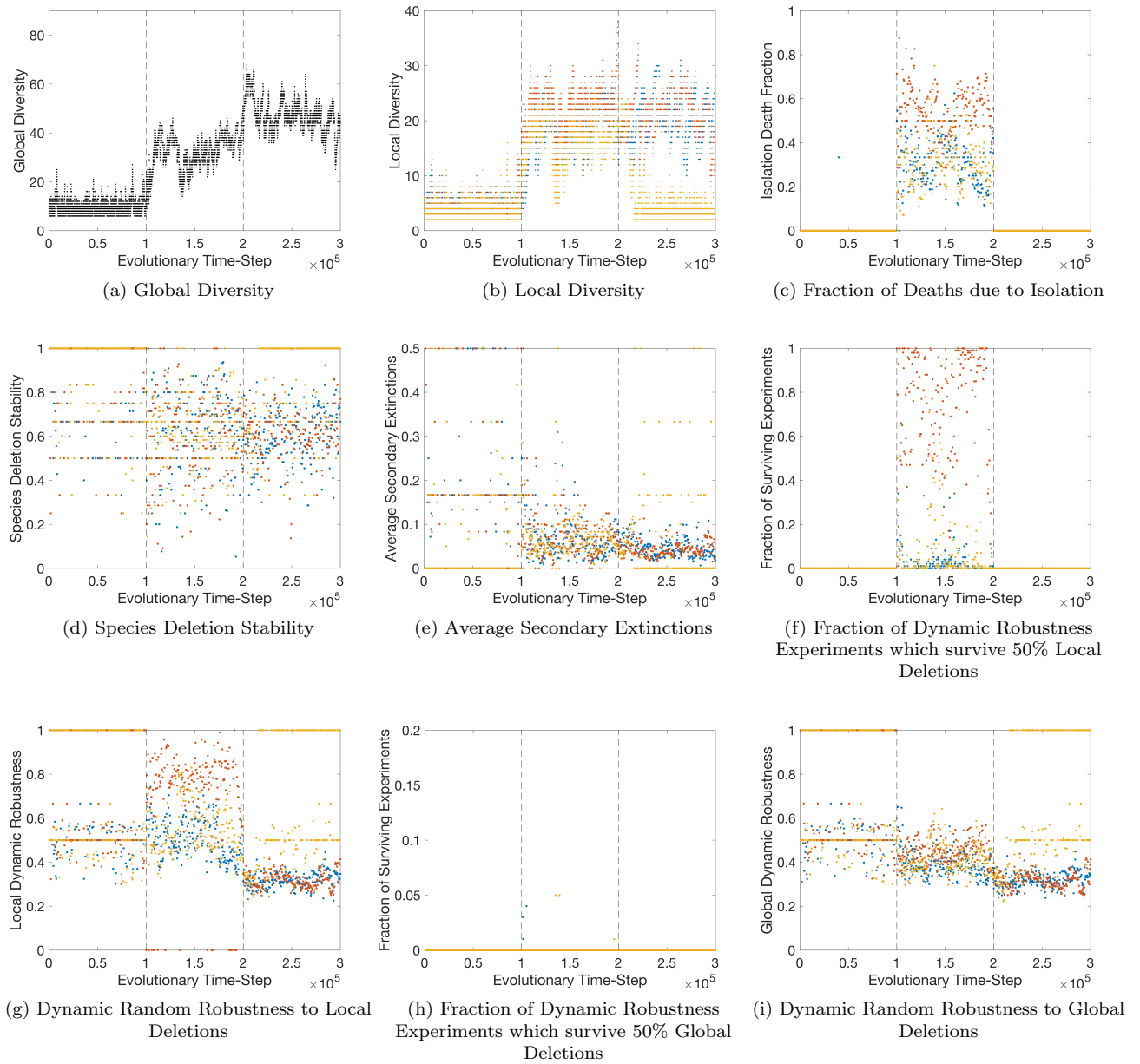
(a) Global Diversity

(b) Local Diversity

(c) Fraction of Deaths due to Isolation

(d) Species Deletion Stability

(e) Average Secondary Extinctions

(f) Fraction of Dynamic Robustness Experiments which survive 50% Local Deletions

(g) Dynamic Random Robustness to Local Deletions

(h) Fraction of Dynamic Robustness Experiments which survive 50% Global Deletions

(i) Dynamic Random Robustness to Global Deletions

Figure 12: Diffusion V2 Dynamic Stability Analysis
Blue = Cell 1
Red = Cell 2
Yellow = Cell 3

(a) Global Diversity

(b) Local Diversity

(c) Fraction of Deaths due to Isolation

(d) Species Deletion Stability

(e) Average Secondary Extinctions

(f) Fraction of Dynamic Robustness Experiments which survive 50% Local Deletions

(g) Dynamic Random Robustness to Local Deletions

(h) Fraction of Dynamic Robustness Experiments which survive 50% Global Deletions

(i) Dynamic Random Robustness to Global Deletions
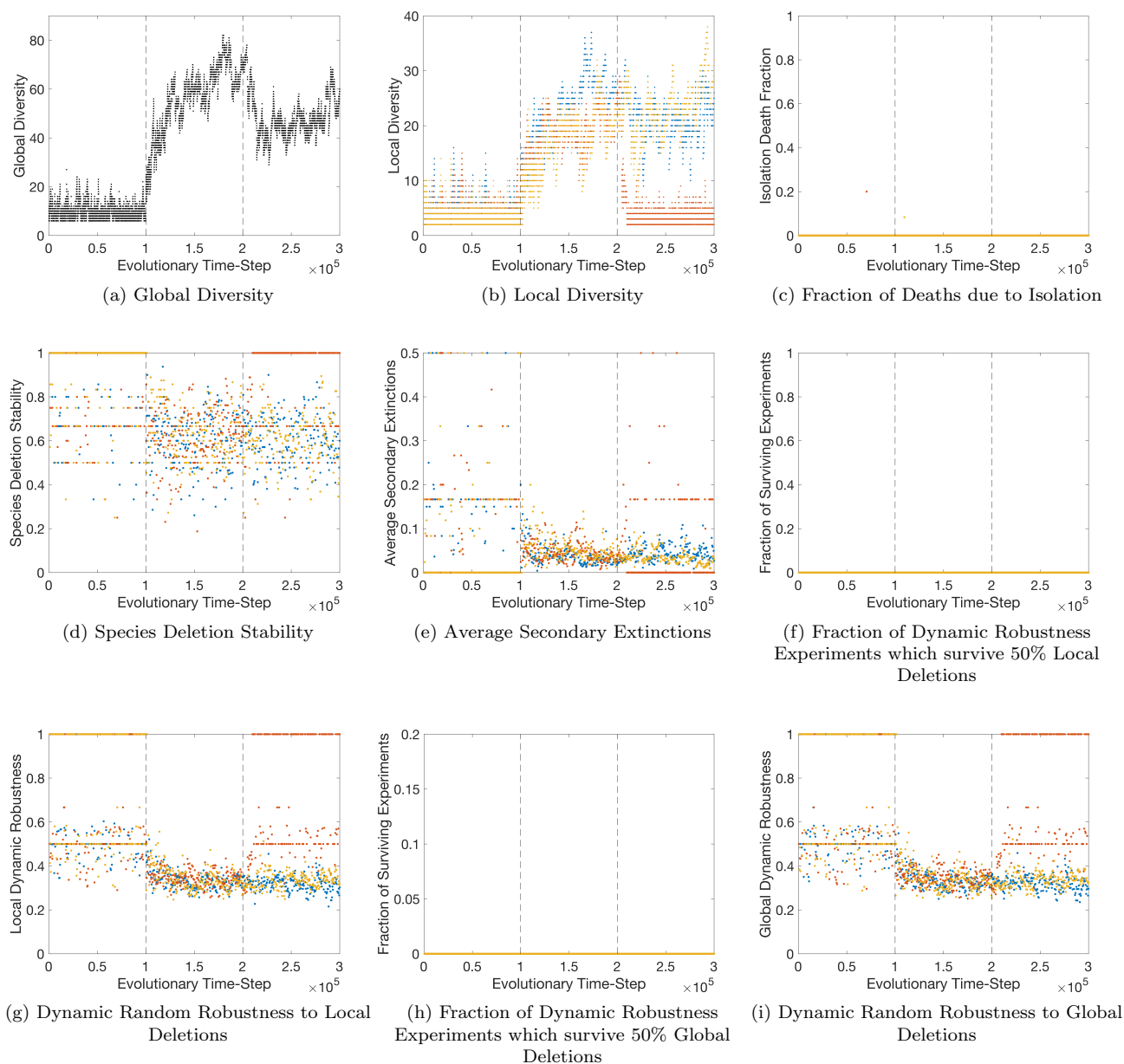
Figure 13: Adaptive Migration V2 Dynamic Stability Analysis
Blue = Cell 1
Red = Cell 2
Yellow = Cell 3

6.1. Observations

As before, adaptive migration increases global diversity the most during migration, as it does not result in homogeneous arrangements of local populations as is the case with constant diffusion migration. In fact, global diversity actually decreases when adaptive migration is switched off (Figure 13(a)). This suggests that whilst other migration schemes have only a temporary usefulness to kick-start diverse local populations, this form of migration has an ongoing, truly positive effect on global diversity. This contrasts with diffusion migration, where switching it off results in between 20 and 50% extinctions in extreme cells (1 and 3), and between 50 and 70% of the central cell (2) going extinct (Figure 12(c)). This indicates that constant diffusion is supplying satellite local populations that are not capable of sustaining themselves, whilst adaptive migration is actually benefitting the established local diversity of the cells as the populations do not require continued migration. Despite these differences, we observe almost identical patterns for species deletion stability and average secondary extinctions between the two schemes (Figure 12(d),(e), Figure 13(d),(e)). This means that the local networks that remain after isolation (large for adaptive migration and small for diffusion) display similar patterns for these stability properties. Thus, whilst adaptive migration strengthens the inherent diversity of the cell, it does not have any effect on the relative species deletion stability of the sustainable part of the ensemble compared to diffusion - so in this model, the choice of dispersal mechanisms influence intrinsic diversity but not this form of stability.

For how the spatial component interacts with our other measure of stability, we consider the two forms of dynamic robustness. The robustness to local and global deletions follow a similar pattern for adaptive migration (Figure 13(g) and (i)): decreasing during the period when migration is occurring and then during the final part of the simulation remaining lower than it was before migration. This indicates that the effect is due not to movement happening during the deletion process, but to the inherent properties of the local food webs during this period of the simulation: adaptive migration is resulting in higher-diversity food webs which therefore have lower robustness. This negative correlation between diversity and robustness was confirmed for the Webworld model in our previous study [AMG19]. In this way, migration is influencing the long-term properties of the metacommunity. However, for diffusion migration, whilst robustness to global deletions follows a similar pattern, the robustness to local deletions is quite different. In this case, the frequent movement of species is directly impacting the robustness experiment, as local populations are being replenished between deletion events which results both in experiments being survived altogether (Figure 12(f)), and in the robustness of successful experiments being much higher during the migration period (Figure 12(g)). Cell 2 benefits the most from this effect, as it is supported by the flow of biomass from two rather than one cells feeding in to it to replenish deleted local populations. For both simulations there were no cases of a local cell remaining robust against global deletions of species. While this may seem obvious, we could not *a priori* rule out the possibility that deleting species x in all cells would allow species y to establish a local population in the cell under consideration when it could not do so otherwise.

7. 25-cell system

The final experiment conducted is a preliminary for future research, that could use a spatial version of Webworld for sophisticated eco-evolutionary simulations on a large scale, modelling the development of life across one or more continents with unique weather, temperature, resources and varying the degree to which routes between local environments are traversable. We perform five simulations on a two-dimensional grid of 5×5 cells and with 1 000 000 evolutionary timesteps. In this case, we start with a unique resource in every cell, however we have only one initial species in cell $(1, 1)$. Movement using the adaptive migration scheme between adjacent (non-diagonal) cells is enabled from the very beginning, with $\phi = 25$ so that in this setup the whole remaining population will leave a central cell connected to four others if the population has decreased by $1/2$ or more, because one quarter will go to each neighbouring cell. Each cell has homogeneous parameters $R = 1 \times 10^4$ and $c = 0.7$. The data from one such simulation is presented here, while the corresponding results for the other four simulations can be found in the supplementary material.
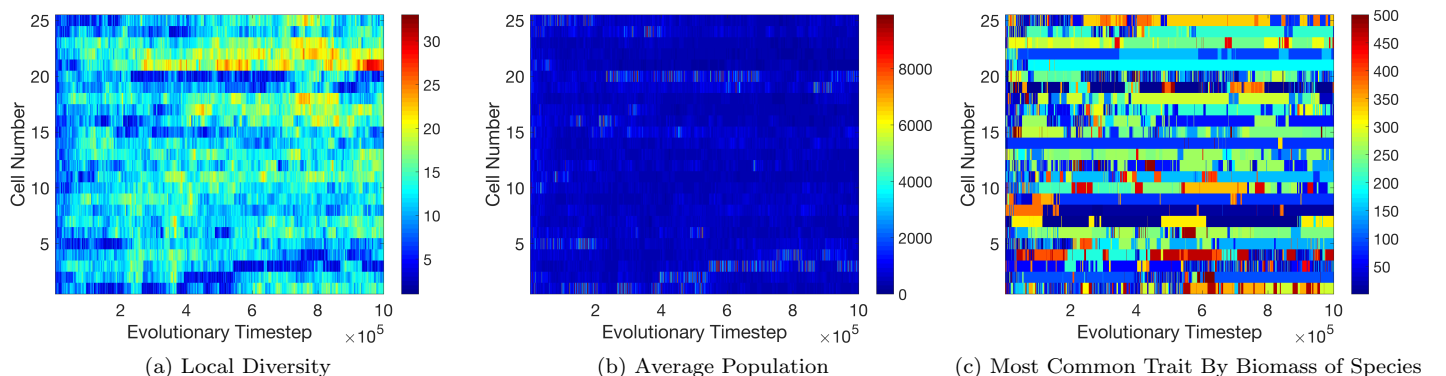

(a) Local Diversity   (b) Average Population   (c) Most Common Trait By Biomass of Species

Figure 14: 25-cell System Cell Properties

7.1. Observations

The choice of adaptive migration, as in Section 5, has successfully resulted in the emergence of diverse and distinct local food webs when combined with spatially-heterogeneous environments even when the food webs co-evolve from the very beginning of the simulation. This is confirmed from the diversity time-series: global diversity is far greater than the average local diversity throughout the simulation (Figure 15(a)), and we see that around 80% of non-resource species in each cell are not present in any other cells (Figure 15(b)). We note that previous studies utilising adaptive migration could only construct distinct networks if they were allowed to evolve in isolation for an initial period [AWRD15], as these particular experiments considered homogeneous environmental parameters and only two patches. Furthermore, the computation time for these experiments are reasonable compared to the other simulations presented in this study, making adaptive migration a suitable candidate for future large-scale research.

What are the characteristics of the food webs that develop in such a large metacommunity? Diversity is highly variable (Figure 14(a)), and spatial topology is influential in the sense that the constitution of neighbouring cells has some significance in

(a) Local Diversity (Red), Global Diversity (Blue)

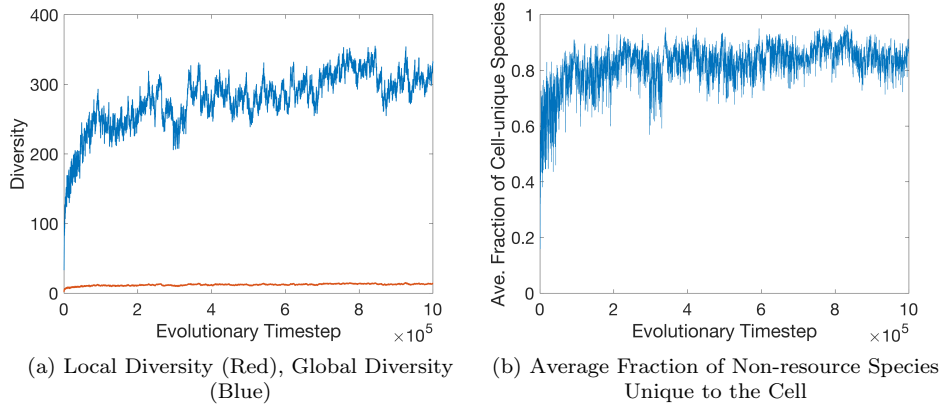(b) Average Fraction of Non-resource Species Unique to the Cell

Figure 15: 25-cell System Average Time-series

such a large system. Cell 21 has the greatest local diversity towards the end of the simulation, and is a part of a ring of adjacent cells 16, 17, 21 and 22 that all have above-average diversity for a long period. In addition, we can see that in many cells, a single trait (but not necessarily the same one between cells) is dominant by biomass amongst non-resource species for very long times (Figure 14(c)). In particular, consider cell 21 again. A single trait is dominant for almost the entire simulation, during which the diversity fluctuates between about 13 and 33. The question then is: is this because of a single, well-established species with huge population, or are there many species sharing this particularly strong trait? Reconstructing the local food web in this cell at the end of the simulation, it has 25 non-resource species with three trophic levels and a fairly even spread of population sizes. The most-populous species has a population size less than 20% greater than the second-largest. This structure does not suggest one dominant species.

Studying the phylogenetic tree of the metacommunity (Figure 16(a)), it appears that some species do persist for large

(a) Ancestry of Final Food Web
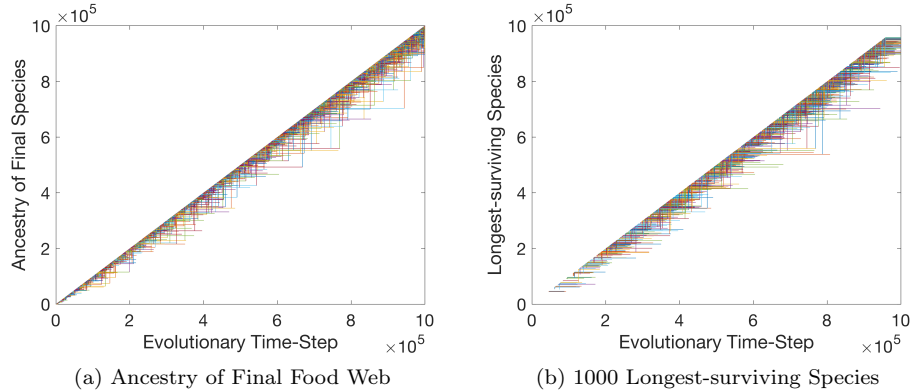
(b) 1000 Longest-surviving Species

Figure 16: Phylogeny for 25-cell system

portions of the simulation. However, if we only show the ancestral tree of the surviving species there could be other species who eventually died out, but for long periods dominated with a large population and so had one of their traits as the dominant trait of a cell. Therefore, we also plot the lifespans of the 1000 longest-surviving species (Figure 16(b)). We see from this that the longest surviving species had a lifespan of 269,398 evolutionary timesteps - approximately one quarter of the entire simulation. Since a few species last for moderately long times, it seems probable that the dominant trait by biomass is one shared by multiple basal species who occasionally are replaced by another slightly better-adapted basal species. Our previous study [AMG19] confirms that there is more trait overlap on the first trophic level (up to 60%) and we know that they have collectively much larger populations than species on higher trophic levels. Furthermore, species on this trophic level are directly influenced by the only permanent feature of the cell, which is the trait arrangement of the resource, and in our previous paper we concluded that this has a strong influence on the traits that are popular in the cell throughout the simulation [AMG19]. Therefore the network of networks that emerge from this spatial eco-evolutionary simulation reflects both the influence of the local factors of each environment (the unique local resource impacts which traits will flourish in that cell) and the role of adaptive migration as these 25 spatially-heterogeneous food webs co-evolved from a single initial species occupying just one corner patch.

8. Conclusions

In this paper, we have developed a spatial extension of the popular eco-evolutionary Webworld model, and determined that it is robust against a number of factors. Temporal variation of the resource's size R during the ecological loop did not have much impact with the low amplitudes we tested, while spatial topology is not too important for small networks of two or three cells but facilitates distinct compartments in large metacommunities with adaptive migration.

This study has highlighted the interplay between the mechanism used to implement migration and properties of the local habitats in constructing diverse metacommunities. Using a stochastic dispersal scheme, occassionally displacing relatively large local populations has an extremely restrictive outcome and results in poorer local diversity than when the networks are constructed in isolation. When using constant diffusion migration, a high rate of movement between cells with different local resources is disruptive - resulting in synchronisation and significantly reduced global diversity (Figure 8(a),(b)) as observed in other studies - but could be beneficial if it was only permitted for a temporary period or at a very low rate. However, when cells with homogeneous resources are allowed to evolve in isolation first, they can easily maintain more distinct food webs when coupled by diffusion migration. However, the degree of synchronisation between sites with heterogeneous resources can also be partly reduced by increasing the number of cells and choosing less-connected spatial topologies.

Adaptive migration is the most effective at promoting both local and global diversity, with clear and consistent positive effects on local food webs with differing resources whether enabled from the beginning or after the networks have been allowed to evolve in isolation (Figure 8(c),(d), and 13(a)). Using this mechanism in a 5×5 network of cells with heterogeneous local resources, we simulated the co-evolution of 25 distinct communities from a single non-resource species in only one of the cells. As seen in other models, stability can be improved by constant migration providing rapid rescue effects (diffusion improves dynamic robustness), whilst species deletion stability was not improved. Adaptive migration did not display this quality, but rather created larger established networks that could continue without migration, and possessed the same levels of relative species deletion stability.

Combining explicit spatial modelling with trait-based eco-evolutionary models is a natural extension of the currently existing computational models, and one that is still relatively unexplored. Future research could involve allowing spatial factors to affect species mortality and efficiency, and we intend to study a form of stochastic migration which allows properties of the species other than population size to influence its propensity for traversing between cells. For example, it could be interesting to consider movement speed as a continuous trait subject to mutation. However, from the results presented here, we conclude that spatial models which either feature temporary periods of migration that only allow very small fractions of populations to migrate on rare occasions, or where movement is only in response to environmental pressure, are the most conducive to promoting species diversity at both the local and global levels. Furthermore, these results reinforce the destructive effects of species displacement: coercing large fractions of local populations to leave the local ecosystems in which they have becomes established, and introducing them to other sites, consistently restricts the local and global diversity of the metacommunity. Preventing this is therefore an essential element of promoting conservation and sustainability. In the future, we will focus on using large-scale spatially-heterogeneous metacommunities to simulate the spread of life over continents and the emergence of distinct ecosystems that are adapted to their local environments. Such models could be used in order to test the effect of climate change and habitat loss: such as what happens if all of the species in a certain cell are displaced, or the resource or other environmental parameters in one cell were to change unexpectedly.

9. Funding

[AMG19] Gavin M Abernethy, Mark McCartney, and David H Glass. The robustness, link-species relationship and network properties of model food webs. *Communications in Nonlinear Science and Numerical Simulation*, 70:20 − 47, 2019.

[ARRDG15] K. T. Allhoff, D. Ritterskamp, B. C. Rall, B. Drossel, and C. Guill. Evolutionary food web model based on body masses gives realistic networks with permanent species turnover. *Scientific Reports*, 5:10955 EP −, 06 2015.

[AWRD15] Korinna T. Allhoff, Eva Marie Weiel, Tobias Rogge, and Barbara Drossel. On the interplay of speciation and dispersal: An evolutionary food web model in space. *Journal of Theoretical Biology*, 366:46 − 56, 2015.

[BDA17] Lev Bolchoun, Barbara Drossel, and Korinna Theresa Allhoff. Spatial topologies affect local food web structure and diversity in evolutionary metacommunities. *Scientific Reports*, 7(1):1818, 2017.

[CHM98] Guido Caldarelli, Paul G. Higgs, and Alan J. McKane. Modelling coevolution in multispecies communities. *Journal of Theoretical Biology*, 193(2):345 − 358, 1998.

[DALP09] Andy Dobson, Stefano Allesina, Kevin Lafferty, and Mercedes Pascual. The assembly, collapse and restoration of food webs. *Philosophical Transactions of the Royal Society B: Biological Sciences*, 364(1524):1803–1806, 2009.

[DHM01] Barbara Drossel, Paul G. Higgs, and Alan J. McKane. The influence of predator-prey population dynamics on the long-term evolution of food web structure. *Journal of Theoretical Biology*, 208(1):91 – 107, 2001.

[DMQ04] Barbara Drossel, Alan J. McKane, and Christopher Quince. The impact of nonlinear functional responses on the long-term evolution of food web structure. *Journal of Theoretical Biology*, 229(4):539 – 548, 2004.

[Dun06] Jennifer A. Dunne. The network structure of food webs. *Ecological networks: linking structure to dynamics in food webs*, pages 27–86, 2006.

[Fro92] Jan Froyland. *Introduction to chaos and coherence*. CRC Press, 1992.

[GD08] Christian Guill and Barbara Drossel. Emergence of complexity in evolving niche-model food webs. *Journal of theoretical biology*, 251(1):108–120, 2008.

[HCM91] Michael P. Hassell, Hugh N. Comins, and Robert M. May. Spatial structure and chaos in insect population dynamics. *Nature*, 353(6341):255–258, 1991.

[HD17] Michaela Hamm and Barbara Drossel. Habitat heterogeneity hypothesis and edge effects in model metacommunities-marked manuscript. *Journal of Theoretical Biology*, 2017.

[HGHL10] Céline Hauzy, Mathias Gauduchon, Florence D Hulot, and Michel Loreau. Density-dependent dispersal and relative dispersal affect the stability of predator–prey metacommunities. *Journal of theoretical biology*, 266(3):458–469, 2010.

[HMW96] RJ Hendry, JM McGlade, and J Weiner. A coupled map lattice model of the growth of plant monocultures. *Ecological modelling*, 84(1):81–90, 1996.

[HZ16] Tousheng Huang and Huayong Zhang. Bifurcation, chaos and pattern formation in a space-and time-discrete predator–prey system. *Chaos, Solitons & Fractals*, 91:92–107, 2016.

[HZY+17] Tousheng Huang, Huayong Zhang, Hongju Yang, Ning Wang, and Feifan Zhang. Complex patterns in a space-and time-discrete predator-prey model with beddington-deangelis functional response. *Communications in Nonlinear Science and Numerical Simulation*, 43:182–199, 2017.

[LHM+04] Mathew A Leibold, Marcel Holyoak, Nicolas Mouquet, Priyanga Amarasekare, Jonathan M Chase, Martha F Hoopes, Robert D Holt, Jonathan B Shurin, Richard Law, David Tilman, et al. The metacommunity concept: a framework for multi-scale community ecology. *Ecology letters*, 7(7):601–613, 2004.

[LL05] Nicolas Loeuille and Michel Loreau. Evolutionary emergence of size-structured food webs. *Proceedings of the National Academy of Sciences of the United States of America*, 102(16):5761–5766, 2005.

[LL08] Nicolas Loeuille and Mathew A. Leibold. Evolution in metacommunities: On the relative importance of species sorting and monopolization in structuring communities. *The American Naturalist*, 171(6):788–799, 2008. PMID: 18419341.

[Llo95] Alun L. Lloyd. The coupled logistic map: a simple model for the effects of spatial heterogeneity on population dynamics. *Journal of Theoretical Biology*, 173(3):217 – 230, 1995.

[LM08a] Carlos A. Lugo and Alan J. McKane. The characteristics of species in an evolutionary food web model. *Journal of Theoretical Biology*, 252(4):649 – 661, 2008.

[LM08b] Carlos A. Lugo and Alan J. McKane. The robustness of the webworld model to changes in its structure. *Ecological Complexity*, 5(2):106 – 120, 2008. Current Food-Web Theory.

[MAGM16] Rory Mullan, Gavin M. Abernethy, David H. Glass, and Mark McCartney. A single predator multiple prey model with prey mutation. *Communications in Nonlinear Science and Numerical Simulation*, pages –, 2016.

[May09] Robert M May. Food-web assembly and collapse: mathematical models and implications for conservation. *Philosophical Transactions of the Royal Society of London B: Biological Sciences*, 364(1524):1643–1646, 2009.

[McC00] Kevin S. McCann. The diversity-stability debate. *Nature*, 405(6783):228–233, 05 2000.

[McK04] Alan J. McKane. Evolving complex food webs. *The European Physical Journal B - Condensed Matter and Complex Systems*, 38(2):287–295, 2004.

[ML02] Nicolas Mouquet and Michel Loreau. Coexistence in metacommunities: the regional similarity hypothesis. *The American Naturalist*, 159(4):420–426, 2002.

[ML03] Nicolas Mouquet and Michel Loreau. Community patterns in source-sink metacommunities. *The american naturalist*, 162(5):544–557, 2003.

[QHM02] Christopher Quince, Paul G. Higgs, and Alan J. McKane. Food web structure and the evolution of ecological communities. In Michael Lässig and Angelo Valleriani, editors, *Biological Evolution and Statistical Physics*, volume 585 of *Lecture Notes in Physics*, pages 281–298. Springer Berlin Heidelberg, 2002.

[QHM05a] Christopher Quince, Paul G. Higgs, and Alan J. McKane. Deleting species from model food webs. *Oikos*, 110(2):283–296, 2005.

[QHM05b] Christopher Quince, Paul G. Higgs, and Alan J. McKane. Topological structure and interaction strengths in model food webs. *Ecological Modelling*, 187(4):389 – 412, 2005.

[RIAI08] A G Rossberg, R Ishii, T Amemiya, and K Itoh. The top-down mechanism for body-mass-abundance scaling. *Ecology*, 89(2):567–580, Feb 2008.

[SBV92] Ricard V. Solé, Jordi Bascompte, and Joaquim Valls. Nonequilibrium dynamics in lattice ecosystems: Chaotic stability and dissipative structures. *Chaos*, 2(3):387–395, 1992.

[TD18] Tatjana Thiel and Barbara Drossel. Impact of stochastic migration on species diversity in meta-food webs consisting of several patches. *Journal of theoretical biology*, 443:147–156, 2018.